Atmospheric Environment 288 (2022) 119324

Contents lists available at ScienceDirect

Atmospheric Environment

journal homepage: www.elsevier.com/locate/atmosenv

Source appointment of volatile organic compounds and evaluation of anthropogenic monoterpene emission estimates in Atlanta, Georgia

Yuyang Peng [a], Asher P. Mouat [a], Yongtao Hu [a], Meng Li [c,d], Brian C. McDonald [d], Jennifer Kaiser [a,b,*]

[a] School of Civil and Environmental Engineering, Georgia Institute of Technology, Atlanta, GA, 30332, USA
[b] School of Earth and Atmospheric Sciences, Georgia Institute of Technology, Atlanta, GA, 30332, USA
[c] Cooperative Institute for Research in Environmental Sciences, Univ. of Colorado, Boulder, CO, 80309, USA
[d] Chemical Science Laboratory, NOAA Earth System Research Laboratory, Boulder, CO, 80305, USA

HIGHLIGHTS

- PTR-ToF-MS VOC measurements over 7 months in 2020 resolved into 8 factors via NNMF.
- Strong seasonality trends in biogenic and secondary factors, minimum seasonality in anthropogenic factors.
- 26% in summer and 53% in winter of all monoterpenes are anthropogenic in Atlanta.
- NEI underestimates anthropogenic monoterpenes by up to 70%, FIVE-VCP agrees better with observations.
- Anthropogenic monoterpenes may significantly impact summertime urban SOA formation.

ARTICLE INFO

Keywords:
Monoterpenes
Emission source analysis
VCPs
VOC seasonal Trends
SE US
Urban air quality

ABSTRACT

Emissions of monoterpenes from volatile chemical products (VCPs) have been shown to contribute substantially to secondary organic aerosol (SOA) formation in a number of cities across the US. In the southeast US (SE US), monoterpenes are the dominant precursor to SOA production. Previous studies have assumed that monoterpenes are primarily biogenic in origin. We examine that assumption here using a total of nine months of volatile organic compound (VOC) observations spanning across 2020 and 2021 which are made via proton-transfer-reaction time-of-flight mass spectrometer (PTR-ToF-MS) in Atlanta, Georgia. The dataset is resolved via non-negative matrix factorization (NNMF) into two biogenic, four anthropogenic, and two secondary factors. NNMF results show that VCP sources contribute to 0.28 ± 0.17 ppb of monoterpenes, or about 26% of all monoterpenes in the summer and 53% in the winter. Interannual comparison suggest minimum impact of the COVID-19 pandemic on atmospheric VOC composition in Atlanta during the second half of 2020. Comparison of NNMF anthropogenic monoterpenes-to-benzene ($[M_{anthro}/B]$) and anthropogenic-to-total monoterpenes ($[M_{anthro}/M_T]$) ratios with emission ratios in the National Emission Inventory 2016v1 modeling platform (NEI16) and Fuel-Based Inventory of Vehicle Emissions and Volatile Chemical Products (FIVE-VCP) suggests that NEI16 underestimates anthropogenic monoterpene emissions by as much as 70% in Atlanta. FIVE-VCP estimates higher anthropogenic monoterpene emissions than NEI16 and provides better agreement with observations, especially during winter months. Anthropogenic monoterpenes may impact as much as 17% of total summertime SOA formation in Atlanta and the SE US, with potential additional influence of limonene from anthropogenic monoterpene sources due to its higher reactivity and SOA yield potential.

* Corresponding author.School of Civil and Environmental Engineering, Georgia Institute of Technology, Georgia Tech, Ford ES&T Building, 311 Ferst Dr. NW, Atlanta, GA, 30332, USA
E-mail address: Jennifer.kaiser@ce.gatech.edu (J. Kaiser).

https://doi.org/10.1016/j.atmosenv.2022.119324
Received 11 May 2022; Received in revised form 1 August 2022; Accepted 4 August 2022
Available online 9 August 2022

1. Introduction

The oxidation of highly-reactive monoterpenes ($C_{10}H_{16}$) leads to the formation of secondary organic aerosol (SOA) and ozone (O_3), which is enhanced under high concentrations of nitrogen oxides (NO_x) that are typical of major urban areas (Porter et al., 2017; Monks et al., 2015; Butler et al., 2011; Hoyle et al., 2011). In the southeast US (SE US), monoterpenes are the dominant source of organic aerosol, which is the dominant species in fine particulate matter ($PM_{2.5}$) (Zhang et al., 2018). Monoterpene-derived SOA is further enhanced in the SE US due to high NO_x emissions (Fisher et al., 2016; Pye et al., 2015). Accurate representation of VOC emissions, especially monoterpene emissions, is essential for understanding SOA formation and atmospheric reactivity in this region (McGlynn et al., 2021; Xu et al., 2015).

While the biosphere is the primary source of monoterpenes on the global scale (Hantson et al., 2017; Harrison et al., 2013; Sakulyanontvittaya et al., 2008), recent studies have shown that the use of volatile chemical products (VCPs) can lead to significant monoterpene enhancements in the urban environment (Coggon et al., 2021; McDonald et al., 2018). Monoterpenes, especially limonene, are commonly used in fragrances, and have been shown to be an effective VCP tracer given their high correlation with other VCP components such as decamethylcyclopentasiloxane (D5-siloxane) (Gkatzelis et al., 2021a). In Manhattan, NY, the estimated summertime monoterpene flux from VCP sources is comparable to that from a forest of the same size in the SE US (Coggon et al., 2018, 2021). Mobile source emissions continue to decrease in the US due to tightened control measurements over the past few decades (Jiang et al., 2018), and monoterpenes and other anthropogenic VOCs (AVOCs) from VCP sources show increasing prevalence that are underrepresented in current inventories especially in urban areas (de Gouw et al., 2018).

A new emission inventory, the Fuel-Based Inventory of Vehicle Emissions and Volatile Chemical Products (FIVE-VCP) (Coggon et al., 2021; McDonald et al., 2018), estimates much higher VCP emissions than the commonly used US EPA National Emission Inventory (NEI) (USEPA, 2021). Both inventories account for VCPs from various industrial and consumer-based emission sources, although the per-capita emission factors used in FIVE-VCP yield much higher VOC emissions that becomes more pronounced in densely populated urban centers, especially from the following sectors: pesticides, coatings, adhesives, personal care products, and cleaning (i.e., household) products (Qin et al., 2020). The larger contribution of anthropogenic monoterpenes in FIVE-VCP from personal care products and cleaning products drives the discrepancies of monoterpene emission estimates between these two inventories.

Chemical transport model (CTM) simulations estimate that monoterpenes contribute to ~20% of total OA on a regional scale in the SE US (Kim et al., 2015), while local observations in Atlanta indicate a much higher contribution of nearly 50% of all SOA in the summer (Zhang et al., 2018; Xu et al., 2015). The higher relative importance in urban areas can at least partially be attributed to higher NO_x concentrations and higher aerosol yields. Anthropogenic emissions have already been shown to significantly enhance SOA formation of biogenic VOCs (BVOCs) (Shrivastava et al., 2019; Shilling et al., 2013; Weber et al., 2007). The growing body of evidence detailing VCP-related VOC emission suggests high anthropogenic monoterpene emissions may also directly contribute to SOA formation. Xu et al. (2018) have highlighted differences in diurnal cycles of modeled and measured monoterpene-SOA, further accentuating uncertainties in current models and inventories, especially in densely populated regions where VCP emissions would considerably impact the total budget of monoterpenes.

In this work, we evaluate the source apportionment of monoterpenes and other VOCs in Atlanta, Georgia using ambient observations made via proton-transfer-reaction time-of-flight mass spectrometer (PTR-ToF-MS) from June to December 2020. We perform a non-negative matrix factorization (NNMF) analysis to differentiate between biogenic and anthropogenic sources, with a focus on monoterpenes. We compare 2020 and 2021 VOC measurements, meteorological data, traffic data, and NO_x observations to identify potential impacts of the coronavirus disease 2019 (COVID-19) pandemic and changes in travel behavior on our source apportionment and its applicability to "typical" scenarios in non-pandemic years. Finally, we compare NNMF-apportioned VOC/VOC mixing ratios with emission ratios as evaluated in the NEI and the FIVE-VCP, as well as overall anthropogenic-to-biogenic ratios using the Model of Emissions of Gases and Aerosols from Nature (MEGAN) version 2.1 algorithm (Guenther et al., 2006, 2012), to investigate potential impact of anthropogenic monoterpene emissions on inventory estimates and discuss implications on secondary pollutant formation in Atlanta.

2. Materials and methods

2.1. Atlanta VOC measurements

VOC concentrations were measured in Atlanta, Georgia from June 15 to December 30, 2020. The measurement site is located in the most population-dense region of the city, on the roof of the Georgia Institute of Technology Ford building (33.78°N, 84.40°W, 40 m above ground level, Fig. 1). Ambient air was drawn through a 12 m PFTE inlet line at a flow rate of 16.6 slm. A portion of this flow (~50 sccm) was pulled into the inlet of an PTR-ToF-MS 4000 trace VOC analyzer (Ionicon Analytik GmbH, Innsbruck, Austria). The PTR-ToF-MS instrument is described in detail by Jordan et al. (2009). We recorded 1-min average spectra over a mass-to-charge ratio (m/z) range of 18–450 at an electric field strength of E/N = 120 Td. Counts are corrected for instrument transmission and normalized to a hydronium ion (H_3O^+) intensity of 10^7 corrected counts per second.

Instrument sensitivity was determined at the end of the campaign using a gravimetric gas standard containing α-pinene, isoprene, toluene, benzene, acetone, acetonitrile, methyl acetate (MESA International Technologies, Inc., Santa Ana, USA). Four of these species (acetone, isoprene, toluene, and α-pinene) were used to determine instrument transmission. A second standard containing isoprene, pentene, benzene, toluene, and xylene (Airgas USA, LLC, Plumsteadville, USA) was used to ensure instrument stability throughout our sampling period. Calibrations with the second standard were performed on a monthly basis from August through December. As this second standard reached its certification date during our measurement period, we use these during-campaign calibrations only to check instrument stability, and not to define sensitivity. We see a maximum of 24% difference in calibrations between August and December with no significant trend, and thus conclude that the sensitivities obtained using the calibration at the end of the campaign is representative of the entire dataset.

We identify a total of 58 species measured by the PTR-ToF-MS to include in our analysis (Table S2). This includes any VOC species with clearly resolved m/z peaks in our spectra, so long as there is little anticipated relative-humidity dependence in measurement sensitivity and observations were typically above limits of detection. For these additional species, we calculate theoretical sensitivities using methods outlined in Sekimoto et al. (2017). The uncertainty associated with this method is estimated to be ~50%. Additional information on PTR-ToF-MS instrument calibration and sensitivity calculation is provided in the Supplement (Sect. S1).

To ensure that our analysis is representative of any "typical" year and comment on the potential impact of the COVID-19 pandemic and related changes in anthropogenic activities and consequential emission profiles in Atlanta, we also collect VOC data in 2021 at the same site using identical instrument settings. Additional VOCs measurements span from July 24 to September 08, 2021. A separate calibration is performed using the same 7-species standard for the 2021 data, and theoretical sensitivities for other species were calculated using this calibration.

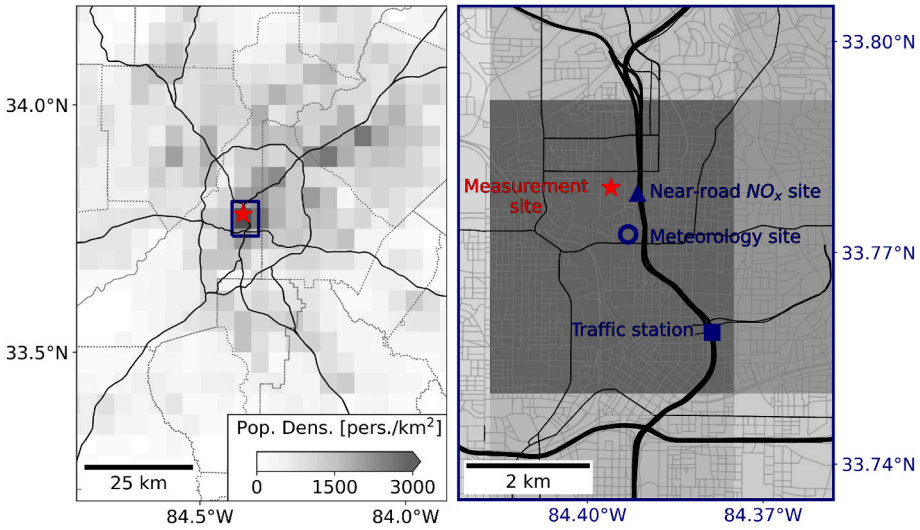

Fig. 1. Map of greater Atlanta (left) and downtown area (right) colored by population density, showing locations of measurement site (red star), meteorology site (blue circle), traffic volume station (blue square), and near-road NO_x site (blue triangle), all within the most-densely populated grid cell. Solid lines represent major (black) and minor (gray) roads. Dotted gray lines represent county borders. (For interpretation of the references to color in this figure legend, the reader is referred to the Web version of this article.)

2.2. Supporting observations

Our VOC source apportionment is supported by observed traffic volumes, meteorological parameters, and near-road NO_x measurements. Traffic volume data are retrieved from the nearby Georgia Department of Transportation Traffic Monitoring Program station (Station ID:121–5474, 33.76°N, 84.38°W) along a major interstate highway, ~2.5 km southeast of the measurement site (Fig. 1, blue square). Meteorological data are from the WeatherSTEM station at the Georgia Institute of Technology Bobby Dodd Stadium (33.77°N, 84.39°W), ~1 km southeast of the VOC measurement site (Fig. 1, blue circle). NO_x data are retrieved from the Georgia Environmental Protection Division NR-GA Tech site (33.78°N, 84.39°W), ~400 m east of the measurement site (Fig. 1, blue triangle).

2.3. NNMF

We use NNMF to determine the source signatures of VOCs in our PTR-ToF-MS data. NNMF requires no prior knowledge of potential sources and can be applied to a large dataset over a long timeframe. We use NNMF as implemented in MATLAB, similar to the method described in Karl et al. (2018). The general formulation of NNMF is:

$$\overleftrightarrow{F} = \overleftrightarrow{W} \times \overleftrightarrow{H} + \overleftrightarrow{r} \quad (1)$$

where $\overleftrightarrow{F}$ represents the measured intensity matrix with dimensions species-by-time (*s-by-t*) comprised of species collected using the PTR-ToF-MS in units of ppbC, which are decomposed into non-negative factors of species fingerprint ($\overleftrightarrow{W}$) and temporal patterns ($\overleftrightarrow{H}$) with dimensions of *s-by-k* and *k-by-t*, respectively, where *k* represents number of factors. The residual matrix is represented as $\overleftrightarrow{r}$. To select the optimal number of factors, we perform NNMF iteratively with different *k* values between 3 and 25, while minimizing the residual matrix $\overleftrightarrow{r}$ and the Bayesian Information Criterion (Stoica and Selen, 2004). We use the NNMF function implemented in MATLAB R2021b 64-bit (version 9.11.0.1837725), with 100 replicates of the factorization algorithm and a maximum iteration of 50 for each replicate and each number of factors. Details on the results of the NNMF analysis, optimization of factors, and reproducibility tests are outlined in the Supplement (Sect. S2).

2.4. Anthropogenic and biogenic inventories

We analyze our NNMF results in the context of two anthropogenic VOC emissions inventories (FIVE-VCP and NEI, 2016v1 platform, hereby shortened as NEI16) and one biogenic emissions model (MEGAN). The FIVE-VCP inventory (McDonald et al., 2018; Coggon et al., 2021) estimates mobile source and VCP emissions using fuel-based methods. Briefly, mobile source emissions are categorized by fuel type (i.e., gasoline and diesel) and engine category (i.e., light-duty vehicles, heavy-duty trucks, and off-road engines) and multiplied with air pollutant emission factors normalized to fuel use. VCP emissions are calculated based on a "bottom up" mass balance method of the petrochemical industry that is based on chemical feedstock data and economic surveys of the chemical industry, which are then spatially allocated based on geolocations for point sources from the 2017 NEI data (NEI17) for industrial VCPs and population density for consumer VCPs. We refer readers to the supplemental text of McDonald et al. (2018) and Coggon et al. (2021), which describe the bottom-up methods in detail for mobile source engines and VCPs. Other anthropogenic emissions are taken from the NEI17 and spatially/temporally allocated using surrogates provided by the NEI. The FIVE-VCP emissions were estimated for the year 2018, to support field measurements made during the Long Island Sound Tropospheric Ozone Study (LISTOS). The data from the FIVE-VCP inventory used in this study are available at https://csl.noaa.gov/groups/csl7/measurements/mobilelab/MobileLabNYICE/DataDownload/wrfchem.php. It has a spatial resolution of 12 km × 12 km, with assumptions of diurnal profiles made to generate hourly emission estimates. Here, we assume the inventory estimates are applicable to the latter half of 2020 without significant impact from the COVID-19 pandemic. Trends in mobile source NO_x emissions and satellite NO_2 observations suggest that emissions had rebounded by July 2020 from COVID-19 lockdown measures, albeit slightly lower than pre-pandemic levels (Harkins et al., 2021; Kondragunta et al., 2021). Furthermore, the interannual comparison detailed in Section 3.3 presents evidence that supports this hypothesis. Considering the atmospheric lifetime of monoterpenes is on the order of a few hours, we find the 12 km resolution to be representative of the measurement site while accounting for potential transport from nearby sources. For our analysis, we use the grid cell centered at 33.80°N, 84.41°W which covers the measurement site and all adjacent supporting observation sites (Fig. 1).

The NEI16 emissions are generated using the HiResX forecasting system, an updated version of the HiRes2 system used to forecast emissions and air quality over the state of Georgia for the year 2020 at a 4 km × 4 km resolution (Hu et al., 2019). HiResX uses the Sparse Matrix Operator Kernel Emissions version 4.6 (SMOKE v4.6) and the NEI 2016v1 platform to generate emissions at this 4 km resolution. The NEI 2016v1 platform is based on the 2014 NEI, version 2 with many sectors

adjusted to 2016 levels locally and nationally as a base emission scenario, available at https://gaftp.epa.gov/Air/emismod/2016/v1/. In addition to 2020 on-road emissions, HiResX also includes 2020 monthly or annual estimates scaled from NEI16 base emission scenario covering these following sectors: non-road fuel, agricultural, residential combustion, non-point oil and gas, other non-point sources, railroads, dust emissions after meteorological adjustments, and low-level point-source emissions. HiResX assumes that NEI16 emissions from these non-traffic sectors are consistent between 2016 and the latter half of 2020 with little impact from COVID-19. We regrid the emission output to 12 km × 12 km to match that of the FIVE-VCP.

For biogenic emissions, we use a simplified emission algorithm of MEGAN v2.1 as outlined in Guenther et al. (2012). Which calculates emission fluxes of a given species i (F_i) from an emission factor at standard conditions (EF_i), activity factors related to temperature ($\gamma_{T,i}$) and solar radiation ($\gamma_{P,i}$), and leaf area index (LAI):

$$F_i = EF_i \times C_{CE} \times LAI \times \gamma_{T,i} \times \gamma_{P,i} \quad (2)$$

C_{CE} is the empirical canopy environment coefficient that sets $\gamma_i = 1$ at standard conditions ($C_{CE} = 0.57$). We use MEGAN v2.1 emission factor with a native resolution of 30 arc seconds available at https://bai.ess.uci.edu/megan/data-and-code/megan21, regridded to 12 km × 12 km to match that of NEI16 and FIVE-VCP used in this analysis. For LAI, we use the BNU MODIS LAI product (Yuan et al., 2011) for 2016 with a resolution of 0.1° × 0.1° (approx. 11 km × 11 km) and 8 days, and assume that the LAI in 2020 is comparable to that of 2016. To calculate the activity factors, we assume that the leaf temperature is equal to ambient temperature, and the photosynthetic photon flux density (PPFD) used to calculate $\gamma_{P,i}$ can be converted directly from measured solar radiation. We assume that ~45% of radiation energy in sunlight is in the visible range between wavelengths 400 and 700 nm useable for photosynthesis, and the energy conversion for the entire spectra is 4.6 μmol photons·J^{-1}, resulting in an overall conversion from solar radiation to PPFD of 1 W m^{-2} ≈ 2.1 μmol photons m^{-2} s^{-1}.

3. Results

3.1. NNMF source apportionment of 2020 VOC observations

Optimizing the NNMF by minimizing the Bayesian Information Criterion (Fig. S2.3) and residual matrix (Fig. S2.4) resulted in a solution containing 8 factors. Fig. 2 presents an abbreviated species profile used for factor identification, and Fig. 3 shows the time series and seasonal diurnal cycles for each factor. The 8 factors include two biogenic factors, four anthropogenic factors (including two traffic-related factors, a cooking and biomass burning factor, and a VCP-dominated factor), and two secondary/other factors (including an acetone-dominated factor and a secondary VOC factor). The identification and characteristics of each factor are described in further detail below. The full factor speciation is provided in the Supplement (Sect. S2.1).

Factor 1 is considered to represent BVOCs co-emitted with, or rapidly produced from, isoprene (C_5H_8). It accounts for the majority (80%) of all observed isoprene, which is a known primary BVOC. The first-generation oxidation products of isoprene, methyl vinyl ketone and methacrolein (MVK/MACR, C_4H_6O), are also primarily allocated to this factor (55%). The factor is most prevalent in warmer summer months (July–August) when isoprene emissions are expected to be high, while decreasing drastically during winter months (November–December) with daily average signals at less than 1% of summertime values. The summertime diurnal cycle is likely affected by both the increasing emission during sunlight hours and the effects of vertical mixing as a resulted of elevated boundary layer height during daytime, which would be responsible for the lower mid-day signal as measured near ground-level. A few other species also slightly correlate with this factor, including monoterpenes ($C_{10}H_{16}$, 6%), sesquiterpenes ($C_{15}H_{24}$, 15%), and acrolein (C_3H_4O, 24%). The correlation between acrolein and this factor is possibly due to similarity in their photo-oxidative temporal patterns, or the fragmentation of propionic acid, methyl propionate, and other secondary species with similar structure to this mass peak in the PTR-ToF-MS instrument (Yuan et al., 2017).

Factor 2 represents BVOCs with less seasonal differences, i.e., other terpenes, identified by its strong representation of monoterpenes (47%) and sesquiterpenes (54%). This factor is characterized by elevated

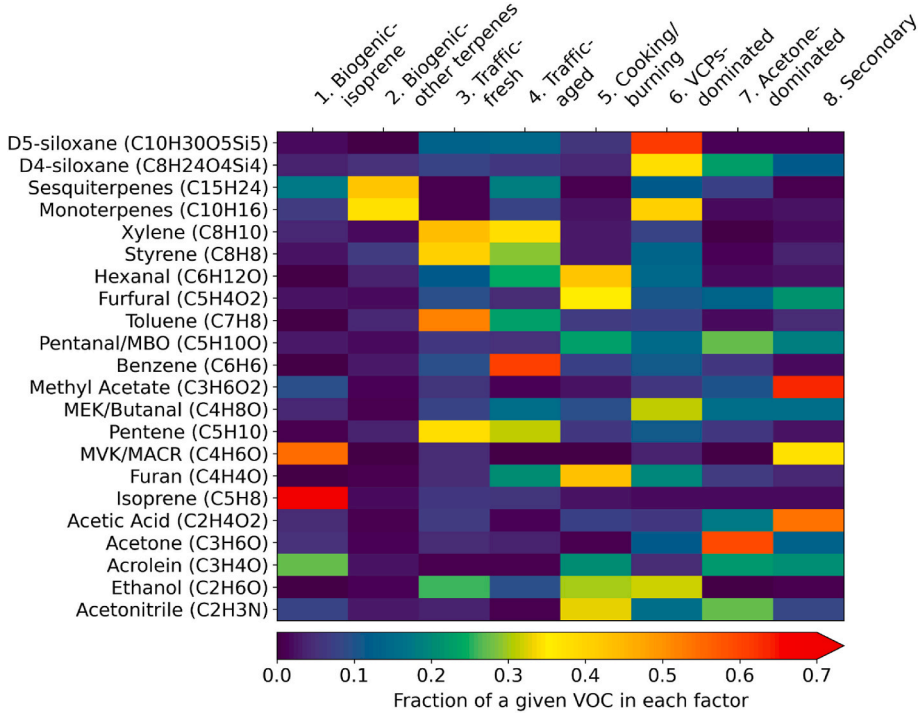

Fig. 2. The 8 NNMF factors and partial contributions from selected tracers, colored by fraction of species in each factor from low (blue) to high (red). The names of the tracers indicate most-likely species with the identified formula. Species are organized in order of descending mass. A version of this figure including all measured species is provided in the Supplement (Fig. S2.1). (For interpretation of the references to color in this figure legend, the reader is referred to the Web version of this article.)

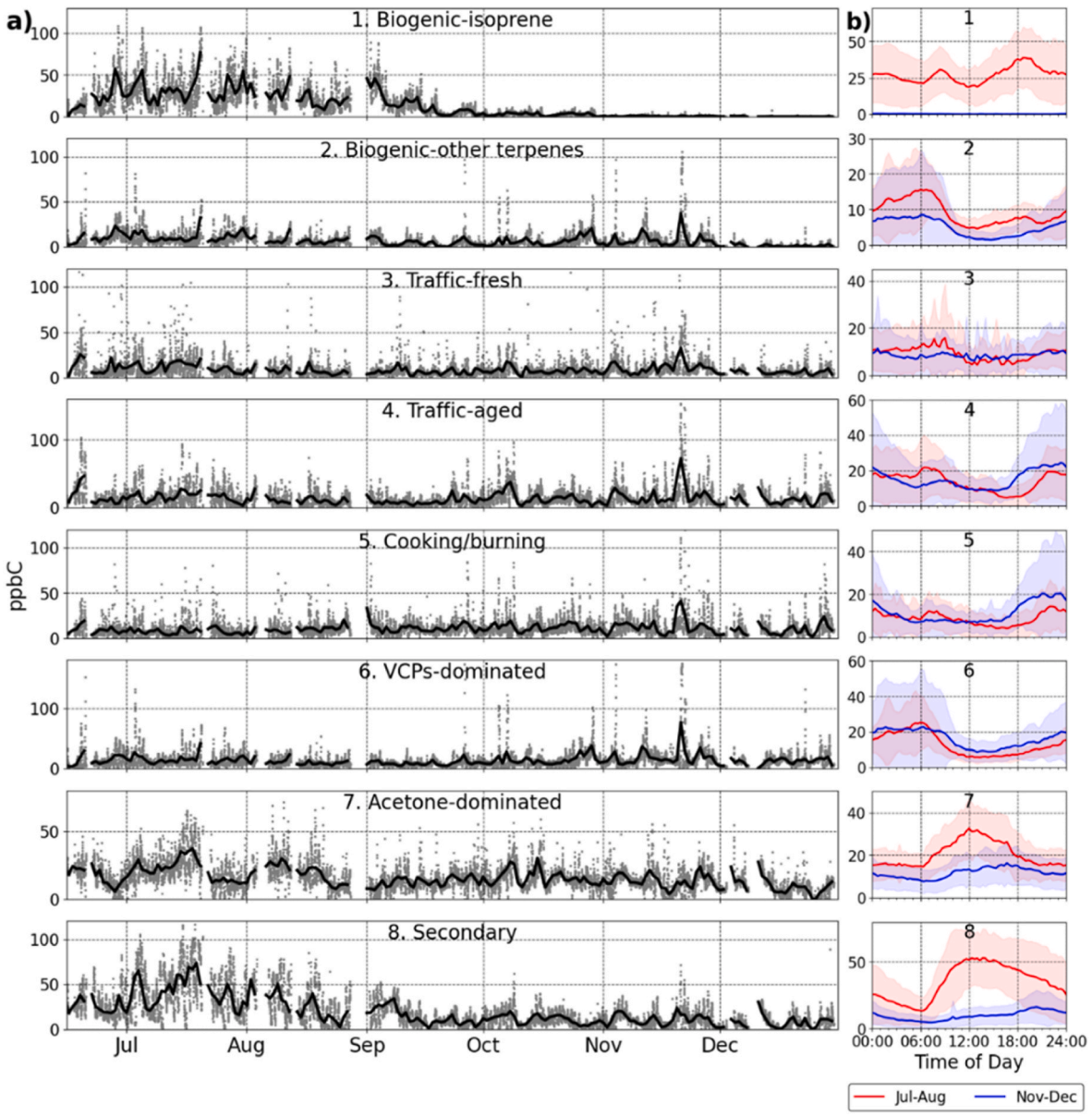

Fig. 3. a) Time series showing data points (gray dots) and daily averages (black line), and b) diurnal cycle of each factor showing summer (Jul.–Aug., red) and winter (Nov.–Dec., blue) patterns. Time series data points are averaged to 20-min resolution for clarity, shaded regions represent standard deviation.

nighttime signals during both seasons, consistent with the light-independent emission characteristics of these terpenes. Unlike factor 1, factor 2 peaks at dawn due to continued emission and decreased oxidation leading to accumulation throughout the night. Measurements of monoterpene mixing ratios from forested areas in the SE US show similar elevated levels at night that peaks in the morning (Qin et al., 2018; Goldan et al., 1995). Wintertime mixing ratios, while nonzero, decrease to about half of summer values, driven by the influence of temperature on biogenic emissions (Fig. S3.1).

Factors 3 and 4 are characterized as "traffic-correlated" factors, as they account for the majority of toluene (C_7H_8), benzene (C_6H_6), xylene (C_8H_{10}), and other aromatic hydrocarbons that are known mobile emission tracers. Both factors combined also contain 26% of the measured ethanol (C_2H_6O) signal, a common fuel additive in the US. The diurnal cycles of factors 3 and 4 are largely consistent between summer and winter, with peaks corresponding to morning and evening rush hours. In addition, the time series of the traffic factors correlate well with local activities around major US holidays, showing elevated levels in the evenings during the weekend before Thanksgiving that coincides with a surge in nearby traffic (Fig. S3.2), although calmer winds and other meteorological factors likely also contributed to this observed increase in traffic-related and other measured VOCs. D5-siloxane ($C_{10}H_{30}O_5Si_5$) and monoterpenes are also slightly apportioned to these factors, though neither is known to be emitted from on-road sources. On-road and VCP emissions have been shown to be temporally correlated based on activity, and commuters in vehicles may also be a significant source of continued VCP emissions (Coggon et al., 2018). These results in our NNMF analysis also suggest VCPs and on-road emissions were not entirely separable due to these suggested correlations.

The distinctions between factors 3 and 4 come from the relative contributions of fast- and slow-reacting species within each factor, particularly toluene and benzene. Factor 3 has a much higher contribution from toluene (42%, vs. 22% for factor 4), while factor 4 has a higher contribution from benzene (53%, vs. 7% for factor 3). The reaction rate constant of toluene with the hydroxyl radical (OH) is almost 5 times higher than that of benzene (Atkinson et al., 2006), resulting in its atmospheric lifetime on the order of a few hours, much shorter than that of benzene at a few days under typical conditions. Other short-lived

aromatics also have higher contribution in factor 3, e.g., xylene at 44% and 36% for factors 3 and 4, respectively. Additionally, factor 3 exhibits uniquely higher variation that are presented as short-lived high concentration episodes ("spikes") in signal during all seasons, especially in daytime, suggesting stronger influence from emission events and faster oxidation. Some of the variation in factors 3 and 4 could also be representative of seasonal variation in mobile source emissions, with evaporative emissions of species such as toluene increasing in warmer months, while benzene and other emissions primarily related to combustion remain relatively constant between the seasons. These findings are consistent with characteristics of fresh and aged primary emission factors previously identified in Beijing in 2010 (Yuan et al., 2012), further indicating influence of atmospheric chemistry on source factorization. Considering the evidence presented in the NNMF, we name factor 3 the "traffic – fresh" factor and factor 4 the "traffic – aged" factor.

Factor 5 represents the cooking and biomass burning sector. It is strongly influenced by furan (C_4H_4O, 46%), furfural ($C_5H_4O_2$, 35%), and acetonitrile (C_2H_3N, 41%), which are all known biomass burning tracers (Müller et al., 2016; Karl et al., 2007; Simoneit, 2002), as well as alkanals such as hexanal ($C_6H_{12}O$, 47%) and pentanal ($C_5H_{10}O$, 22%), which are cooking tracers (Klein et al., 2016; Abdullahi et al., 2013). Acrolein, known for its corrosive and carcinogenic effects, can be emitted from tobacco burning and other combustion processes (Schieweck et al., 2021), also contributes to this factor (21%). In general, biomass burning can be naturally occurring (e.g., wildfires) or human-induced (e.g., prescribed burning), both producing a similar VOC profile of these short-lived oxygenated tracers. Due to the urban location of our measurement site and the minimum seasonality in the factor time series, we can safely presume that most of the VOCs attributed to this factor are of anthropogenic origin.

Factor 6 is considered the VCPs-dominated factor. It is characterized by high contributions of previously identified VCP tracer species such as D5-siloxane (66%) and D4-siloxane ($C_8H_{24}O_4Si_4$, 36%) (Coggon et al., 2018), monoterpenes (38%) (Coggon et al., 2021), ethanol (34%) (de Gouw et al., 2012), acetone (C_3H_6O, 10%) (Brewer et al., 2017), and toluene and other aromatics (6%–11%) (Yuan et al., 2010). These species are known to be directly emitted from VCP sources including solvents, paint, cosmetics, adhesives, and disinfectants, all relevant in various industrial processes, agricultural applications, and urban consumer usage. Other species that slightly correlate with this factor include terpenoids such as camphor ($C_{10}H_{16}O$) and menthone ($C_{10}H_{18}O$) and fragments of species in the PTR-ToF-MS (e.g., C_6H_8 and C_7H_{10}) whose parent ion is likely monoterpenes. Diurnal patterns of this factor display minimum variability between the seasons, peaking in the early morning hours.

Factors 7 and 8 show strong characteristics of secondary VOCs based on speciation and seasonality. Factor 7 is the acetone-dominated factor, marked by high contribution of acetone (66%), and lower amounts of all other species. Acetone in the atmosphere can have both primary and secondary contributions, emitted from industrial sources or produced from oxidation processes of biogenic and anthropogenic emissions (Brewer et al., 2017; Jacob et al., 2002). 2-methyl-3-buten-2-ol (MBO, $C_5H_{10}O$), an isomer of pentanal, also correlates well with this factor, with 32% of the total signal of $C_5H_{10}O$ allocated here. Unlike pentanal, MBO is considered a BVOC that is primarily emitted by coniferous trees and is quickly oxidized by OH with an average lifetime of a few hours (Steiner et al., 2007). Approximately 60% of MBO is oxidized into acetone by OH, which may help explain the high correlation between these two species in this factor. Other VOCs that correlate with this factor include glycolic acid ($C_2H_4O_3$, 34%) and nitrogen-containing species acetonitrile (32%) and acetamide (C_2H_5NO, 43%). Glycolic acid is a second-generation product of isoprene oxidation via MVK/MACR with additional influence from monoterpenes (Link et al., 2021), and acetamide can be strongly influenced by the oxidation of amines in the atmosphere (Borduas et al., 2015). Acetonitrile is relatively inert in the atmosphere with an average lifetime of months to years, and while it is primarily attributed to factor 5 as a traditional biomass burning tracer, evidence of anthropogenic influence from residential and vehicular combustion processes as well as solvent usage may help explain its high correlation with acetone and factor 7 in this NNMF analysis (Huangfu et al., 2021).

Unique events of elevated concentrations of acetone and MBO are captured in factor 7, with varying timespan between a few minutes ("spikes") to days ("plateaus"). An example of a "plateau" happens during mid-July with elevated levels even during nighttime and is reflected in the time series of factor 7 (Fig. 3a). These unique "plateaus" are not as pronounced in any other species in our dataset. The diurnal profile of this factor showing elevated levels mid-day during both seasons suggest that daytime photochemistry may be the dominant source during most days, although sporadic individual "spikes" of acetone are likely results of emission events from different primary sources, such as emissions from nearby buildings and laboratories on campus. While certain species in this factor are known to only come from primary sources (e.g., MBO, acetonitrile), they account for <3% of total VOCs in this factor. Over the course of the entire sampling period, although evidence suggests a stronger influence from primary sources of VOCs in factor 7 than in factor 8, we still expect the majority of VOCs allocated to factor 7 to be from secondary processes.

Factor 8 is identified as the secondary factor. This factor is marked by concentrations of MVK/MACR (42%), glycolic acid (60%), methyl acetate ($C_3H_6O_2$, 67%), acetic acid ($C_2H_4O_2$, 57%), and methylglyoxal ($C_3H_4O_2$, 55%), i.e., oxygenated VOCs whose budgets are dominated by secondary production processes (Paulot et al., 2011; Fu et al., 2008; Biesenthal and Shepson, 1997). This factor has a strong seasonal variation that is driven by secondary VOCs photochemically produced from biogenic emissions, with higher summertime concentrations resulted from both higher biogenic emissions and higher photochemical activity. Unlike factors 1 and 2, diurnal profile of this secondary factor displays a single peak in the middle of the day, consistent with the profile of secondary production that is photochemically driven. Similarities between the temporal and species profiles of factors 7 and 8 may also serve as additional evidence that both factors are driven by secondary processes.

Fig. 4 shows a comparison of the time series of total VOCs measured by the PTR-ToF-MS in each NNMF factor between summer and winter months. The same figure made for the entire 2020 dataset is shown in the Supplement (Fig. S2.2). Certain non-oxygenated VOCs in the atmosphere with lower proton affinity (e.g., alkanes, cycloalkanes, some alkenes) are not measurable thus not included in the total or factorized time series. The stated variability in this following section represents standard deviation of daily average values. The biogenic factors 1 and 2 account for 26.8% of all VOCs in the summer (36.5 ± 17.2 ppbC), decreasing substantially to 6.8% in the winter (5.2 ± 6.4 ppbC). The traffic factors 3 and 4 account for 16.9% of all VOCs in the summer (23.0 ± 10.3 ppbC), and 30.6% in the winter (23.5 ± 16.7 ppbC). The increase in relative contribution is largely a result of decreased biogenic emissions in the winter, while the slightly elevated average signal is likely from longer photochemical lifetimes and lower boundary layer heights rather than increased emissions. Total traffic volumes are relatively consistent between summer and winter months, varying by <10% between summer and winter months (Figure S3.1). Factor 5 (cooking/biomass burning) accounts for a small amount of VOCs during both seasons, at 8.5 ± 3.3 ppbC or 6.2% in summer and 11.1 ± 7.7 ppbC or 14.4% in winter. The increase is largely driven by meteorological conditions similar to the observations in the traffic factors, although increased activity around the major holidays in the US during the winter may also contribute to a portion of this observed seasonality. The VCPs-dominated factor 6 accounts for 9.4% of all VOCs in the summer (12.8 ± 5.9 ppbC), increasing to 21.0% in the winter (16.1 ± 11.0 ppbC). Together, factors 3–6 are comprised of primary AVOCs from various sectors. Total measured AVOCs increased from 44.3 ± 14.3 ppbC (32.5%) to 46.1 ± 33.8 ppbC (66.0%) between summer and winter

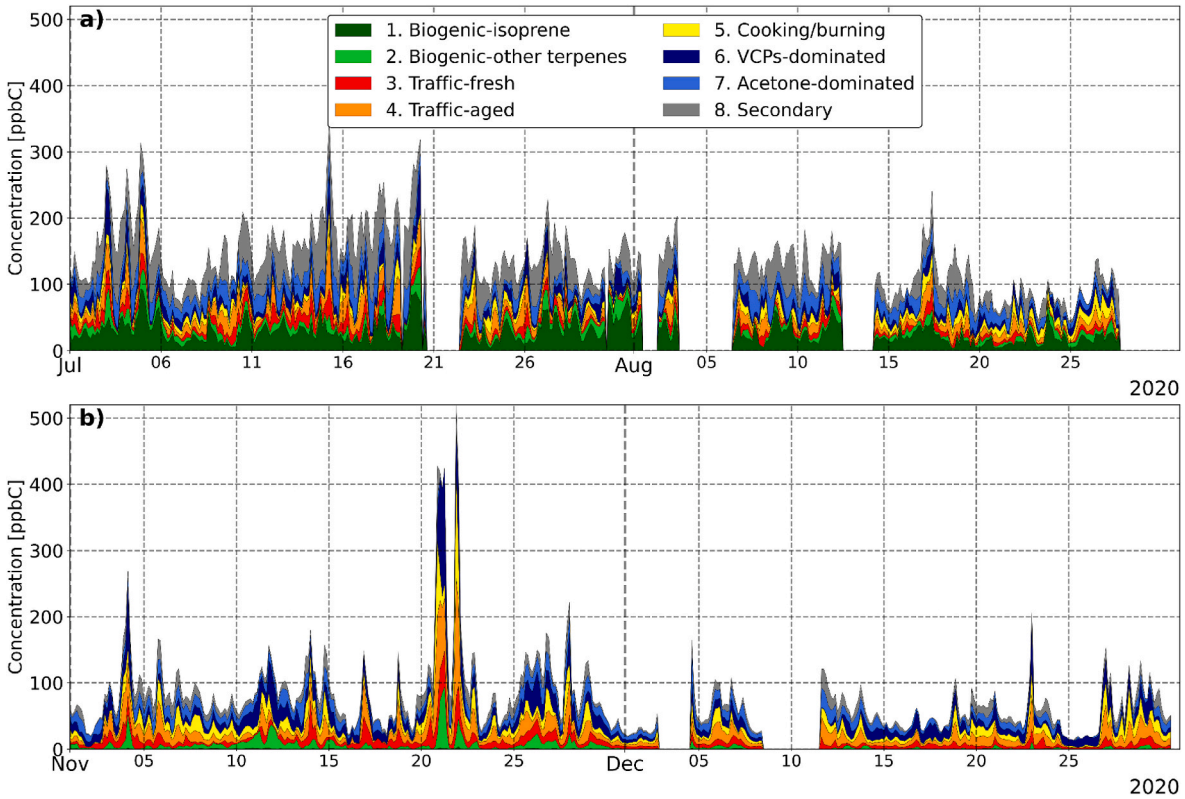

Fig. 4. Time series of VOCs measured by the PTR-ToF-MS in each NNMF factor in (a) July – August and (b) November – December. Data averaged to 3-h temporal resolution for clarity. A version of this figure covering the entire 2020 dataset is included in the Supplement (Fig. S2.2).

months. The increase in concentration between seasons for the anthropogenic factors 3–6 are likely indicating changes in meteorological conditions rather than changes in emission. Factors 7 and 8 are predominantly from secondary sources, and together account for 40.6% (55.3 ± 23.0 ppbC) of total measured VOCs in summer, and 27.2% (20.9 ± 11.1 ppbC) in winter.

Overall, total measured VOCs dropped from 136.2 ± 43.8 ppbC in summer to 76.8 ± 43.6 ppbC in winter. This seasonal difference largely reflects the decrease in biogenic VOCs and secondary species that may be traced back to biogenic sources, which consequently affects the VOC composition as presented above. The significant enhancement of measured VOCs between November 20 and 22, 2020 occurred mostly at night, which is likely a result of increased emission from anthropogenic sources (e.g., traffic) and calm wind conditions leading to accumulation of all VOC species (Figure S3.2). Section S2.4 provides an analysis of variability in NNMF factorization based on 10 additional iterations of the NNMF analysis. We find that these factors are consistently reproduced from our dataset, with an estimated uncertainty of 10% for most species and factors during both seasons.

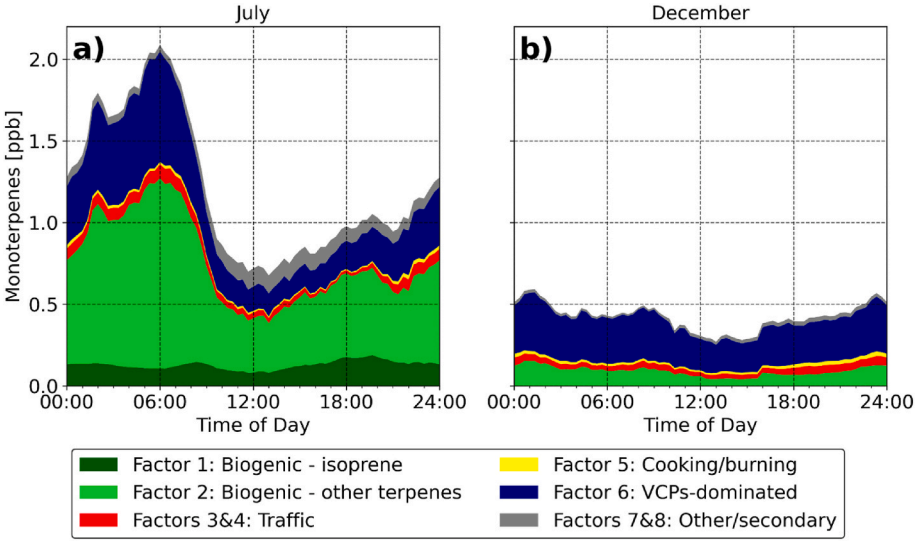

Fig. 5. Seasonal stacked diurnal profiles of monoterpenes in (a) July and (b) December, showing significant decrease in biogenic factors in winter and comparable anthropogenic emissions between seasons including the VCP factor.

3.2. Anthropogenic monoterpenes apportioned via NNMF

With factors 1–8 characterized above, we now consider how monoterpenes are divided into each of the sectors. The portion of monoterpenes in each factor/factor group is shown in Fig. 5. Monoterpene diurnal cycles are carried by the biogenic factors in the summer (0.64 ± 0.34 ppb, or 59%) that are still significant in the winter (0.29 ± 0.36 ppb, 28%). Temperature drives the trend in biogenic monoterpenes that is evident between summer and winter and also between November (0.44 ± 0.43 ppb, 37%) and December (0.09 ± 0.08 ppb, 17%), where daily average temperature drops from 15.5 °C to 8.7 °C. We select July and December as they are the months most representative of this observed reduction in biogenic emissions. Nighttime biogenic contributions can be attributed to the light-independent nature of certain monoterpene emissions from foliage (Guenther et al., 2006, 2012). Peak values of monoterpenes are reached around 6 a.m. local time (LT, UTC+5:00) right before sunrise.

Monoterpenes apportioned to the VCPs-dominated factor 6 remains relatively constant in both summer (0.27 ± 0.13 ppb, 26%) and winter (0.34 ± 0.23 ppb, 53%) with a slightly stronger diurnal variation in the summer. Monoterpenes and D5-siloxane are both emitted from a wide range of personal care products and fragrance additives (Yeoman et al., 2020), and anthropogenic sources of these VCP tracers show direct correlation with population density (Gkatzelis et al., 2021a). Most of D5-siloxane (6.4 ± 3.9 ppt, 66%) is assigned to the VCP factor with minimum seasonal variability. Factor 6 shares a similar diurnal profile with the biogenic factor 2 that peaks in the morning (Fig. 3), and together they make up over 80% of monoterpenes. The seasonality of factor 2 is not present in factor 6, and strong correlations of sesquiterpenes to factor 2 and VCP-related AVOCs (e.g., D5-siloxane) to factor 6 highlight the differences from potential sources between these two factors. Thus, we consider our factorization to be representative of measurement data, sufficiently separating biogenic and anthropogenic monoterpenes. The insignificance of seasonality here also suggests that anthropogenic monoterpenes are largely decoupled from ambient temperature, which may be explained by the fact that most anthropogenic monoterpenes are emitted indoors or from fragranced products on human bodies, both at constant temperatures between seasons. This is in agreement with flux measurements taken at an urban site in Innsbruck, Austria, also suggesting VCPs to be a likely source of urban monoterpenes due to deviation of measurements from biogenic emission parameterizations especially at lower ambient temperatures (Kaser et al., 2022).

Less than 20% of monoterpenes are attributed to the other factors, with about 7% of monoterpenes allocated to the traffic factors, and another 9% to the other/secondary factors. On-road vehicle emission, biomass burning, or secondary processes are not known sources of monoterpenes. The allocation of some monoterpenes to the traffic factors, especially in the winter, is a result of temporal correlation of VCP emissions and mobile source emissions. The correlation between monoterpenes and the traffic factors is similar to that of the D5-siloxane and benzene (Coggon et al., 2018), which is also observed in our dataset with 21% (2.0 ± 1.2 ppt) of D5-siloxane apportioned to the traffic factors. The co-emission of VCP monoterpenes with traffic tracers based on activity especially in the morning is a plausible explanation for this source apportionment, and additional co-emission from car fresheners, street-cleaning, and occupants in vehicles may also enhance this apportionment. In addition, individual "spikes" of high concentration across different species are most-recognized in factors 3 and 4. Two of such "spikes" occurred around November 21 and 22, 2020 (Fig. 4b). These "spikes" are likely results of meteorological effects, i.e., reduced vertical mixing as evident by calmer winds causing an accumulation of VOCs (Fig. S3.2), and are not truly reflective of actual sources during these events. Similarly, the apportionment of monoterpenes to the other factors (cooking/biomass burning, secondary) are also likely due to meteorology and correlation in temporal patterns over the entire sampling period, as neither biomass burning nor secondary oxidation would produce monoterpenes. Condiments and spices from cooking may emit trivial amounts of monoterpenes (Klein et al., 2016), although it is unlikely to make up the entire 3% of all monoterpenes (19 ± 18 ppt) measured by the PTR-ToF-MS. The similarity in diurnal profile and seasonal trends of factors 1 (biogenic – isoprene) and 8 (secondary) may also help explain the apportionment of monoterpenes to the secondary factor, suggesting biogenic influence.

The average apportionment of monoterpenes from VCP sources in Atlanta (26% in summer and 53% in winter) is lower than a similar study conducted in New York City and Boulder, CO, reporting wintertime contribution from VCP sources at 94% and 65%, respectively, of all measured monoterpenes (Gkatzelis et al., 2021b). Monoterpene speciation from forests (Geron et al., 2000) and estimated emission factors based on plant type in the region (Guenther et al., 2006) are higher in the SE US than the other two regions, suggesting regional biogenic emissions likely drive measurable monoterpenes. The extensive foliage coverage of over 50% within the Atlanta city parameters (Merry et al., 2014) with similar plant types as surrounding forests and the estimated monoterpenes atmospheric lifetime of a few hours (Atkinson et al., 2006) may serve as additional evidence of equally strong contribution from local biogenic sources. Warmer temperatures in Atlanta especially in the winter also suggest higher biogenic VOC emission than that in the other two cities. Additional observations of urban-to-rural VOC gradients could help identify sources of monoterpenes in Atlanta and potentially explain the difference compared with other cities. Given the higher year-round biogenic emissions in the SE US and the population density of Atlanta (1360 persons·km^{-2}) standing lower than New York City (10, 800 persons·km^{-2}) but higher than Boulder, CO (180 persons·km^{-2}), our analysis provides a reasonable estimate of source contribution of monoterpenes.

3.3. Comparison between 2020 and 2021

The analysis presented in Section 4 assumes the NNMF source apportionment using 2020 data reflects atmospheric VOC speciation under "typical" scenarios – that is, largely unaffected by the COVID-19 pandemic. Previous literature has highlighted the influence of changes in travel behavior during the pandemic on air quality in Atlanta in early 2020. Huang et al. (2021) show that in March and April, on-road traffic volumes decreased by ~50% compared to 2019 values, and urban NO_2 decreased by ~11%. Kondragunta et al. (2021) estimate on-road emissions in Atlanta decreased 28% in March and April 2020 compared to 2019. By the summertime, traffic had significantly rebounded in Atlanta. Harkins et al. (2021) show that Atlanta has the shortest "lockdown" duration that restricted traffic comparing to other major US cities, and by July, FIVE (i.e., mobile sources only) predicts a small difference in activity (<10%) between the pandemic-impacted and business-as-usual scenarios, and urban VOC emissions across all of US differ by <5%. To evaluate any potential effects of altered anthropogenic emissions scenarios at our specific site, we compare 2020 and 2021 traffic volumes, meteorological conditions, near-road NO_x observations, and summertime VOC observations. Figs. 6 and 7 show the average diurnal cycles for these supporting parameters and VOC measurements. All data have been first averaged to an hourly temporal resolution for consistency and clarity. For the summertime data (July–Aug), we filtered all data to include only days where VOC measurements are also available. This results in 49 available summertime days for 2020 and 33 summertime days in 2021. No VOC observations are available in the winter months of 2021, and data shown include all days in November and December.

In both summer and winter, on-road traffic volumes are relatively consistent between years, but 2020 shows slightly lower traffic volumes during the morning rush hour period. Between 6:00 and 7:00 a.m., which is the focus of our inventory comparison, 2020 summer traffic volumes are 16% lower than 2021 volumes. For the winter months, this

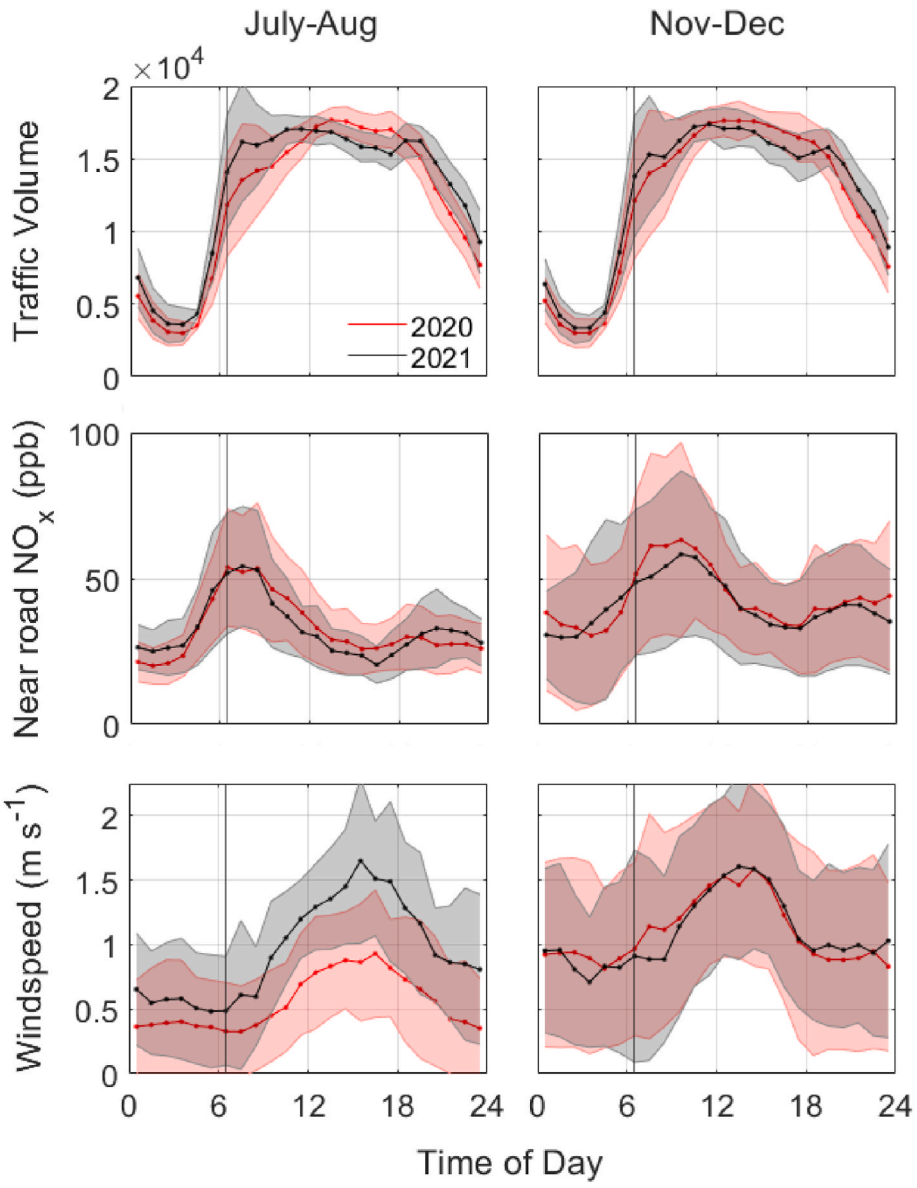

Fig. 6. Hourly diurnal profiles of supporting data, including traffic volume, NO_x, and wind speed between 2020 and 2021, separated by season (left: summer, right: winter). Shaded regions represent standard deviation.

decrease is 12%. Despite this lower traffic volumes, near-road NO_x concentrations are nearly identical, showing no statistically significant difference in either winter or summer months. Similarly, observed summertime benzene mixing ratios appear to be unaffected by the change in traffic volumes. It is possible that total traffic emissions were slightly lower in summer 2020, but lower 2020 windspeeds lead to increased accumulation, such that concentrations where comparable between years. Because the absolute difference in average windspeeds is small (~0.16 m s^{-1}), we assume changes in pollutant transport have a negligible impact on our analysis. In addition, comparison of traffic volume between summer and winter of 2020 (Fig. S3.1) show a difference of <5% in the morning hours, also suggesting that by July, traffic activities at our site have returned to "normal" pre-pandemic levels. The similarities between traffic volumes, near-road NO_x concentrations, and summertime benzene concentrations lead us to conclude that 2020 VOC observations at our site accurately reflect typical mobile-source emissions scenarios.

Changes in other anthropogenic sectors are more difficult to quantify, as localized activity data are not as readily available. Of special interest is the VCP sector, which may be traced by D5-siloxane as suggested by our NNMF analysis. Neither 2020 nor 2021 datasets are calibrated for D5-siloxane using empirical standards, and instrument sensitivity was not constant through the years as determined by the separate calibrations between the years. This leads to higher uncertainty in the interannual comparison shown here. Still, observed morning time siloxanes concentrations are comparable between years, and while afternoon concentrations of D5-siloxane appear to be higher in 2020, this difference is unlikely a reflection of activity levels related to VCP emissions but rather changes in instrument sensitivity that is still within the expected range of uncertainty of D5-siloxane (i.e., ~50% using theoretical sensitivity calculations as shown in Sect. S1).

Our analysis apportions monoterpenes to biogenic and VCP-related sectors. In the summer, any interannual changes in anthropogenic monoterpene emissions may be difficult to extract from the variability driven by biogenic emissions. Still, temperature (not shown) shows no large differences between years, and both isoprene and monoterpenes have consistent concentrations in 2020 and 2021. The consistency between these VOC measurement sets leads us to conclude that 2020 VOC

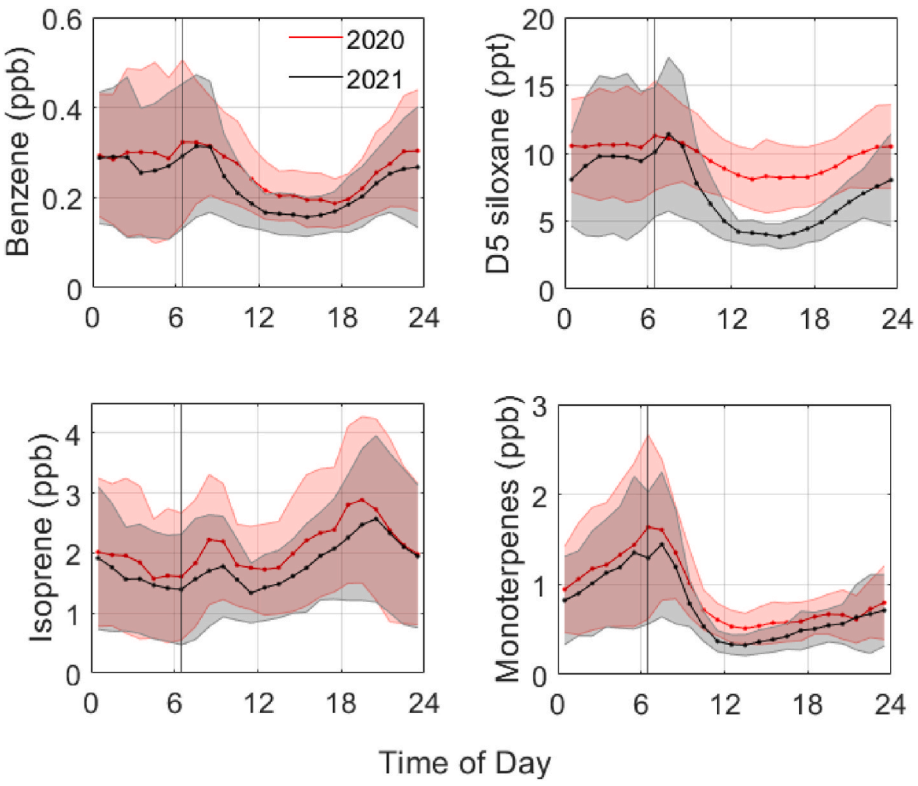

Fig. 7. Summertime hourly diurnal profiles of key VOC tracer species between 2020 (average of 49 days) and 2021 (33 days). Shaded regions represent standard deviation.

observations that missed the most stringent lockdown periods of COVID-19 reflect typical traffic, VCP, and biogenic emission scenarios. Measurements of VOCs in the Los Angeles Basin also show evidence of recovery in AVOC mixing ratios by summer 2020. April and May are most-impacted by the "lockdown" policies imposed in the US, and a >60% increase in afternoon mixing ratios of species associated with gasoline exhaust and evaporation from April–May to June–July suggests increase in activity by summer (Van Rooy et al., 2021). Our comparison is consistent with these findings on VOC composition in urban areas in the US, and we believe that our June–December 2020 measurements are representative of "typical" VOC levels and source apportionment with insignificant impact from the COVID-19 pandemic on anthropogenic activities.

4. Comparison with emission inventories

4.1. Monoterpenes-to-benzene ratios in NEI and FIVE-VCP

Anthropogenic monoterpenes in urban areas are expected to come from fragranced personal care products, a subset of VCPs, with a similar diurnal profile as traffic (Coggon et al., 2021). If we assume that VCP-related monoterpene and traffic-related benzene are co-emitted in the morning, the expected ratio of anthropogenic monoterpenes-to-benzene mixing ratios $[M_{anthro}/B]_{expected}$ can be calculated from the emission ratio ($ER_{M/B}$) photochemical loss rates (Borbon et al., 2013; Warneke et al., 2007):

$$[M_{anthro}/B]_{expected} = ER_{M/B} \times \exp(-(k_{M+OH} - k_{B+OH}) \times [OH] \times \Delta t) \quad (3)$$

where k_{M+OH} and k_{B+OH} represent the bimolecular reaction rate constants of the given VOC with OH. When the emissions are fresh (photochemical age $[OH] \times \Delta t = 0$), $[M_{anthro}/B]_{expected} = ER_{M/B}$. As the air mass ages, $[M_{anthro}/B]_{expected}$ decreases ($k_{M+OH} > k_{B+OH}$). Thus the upper limit of $[M_{anthro}/B]_{expected}$ is $ER_{M/B}$. Observed ratios of anthropogenic monoterpenes-to-benzene that exceeds this limit ($[M_{anthro}/B]_{observed} > ER_{M/B}$) would suggest either (1) an overestimate of benzene emissions, (2) an underestimate of anthropogenic monoterpene emissions, or (3) some biogenic monoterpenes have been misapportioned to the anthropogenic factors in our NNMF likely due to temporal correlations as explained in Section 3.2.

We compare the monthly average values of $[M_{anthro}/B]_{observed}$ with ER_{M/B_NEI} and $ER_{M/B\_FIVE\text{-}VCP}$ during July and December of 2020 (Fig. 8a). This "observed" ratio is derived from the NNMF results, where biogenic monoterpenes have been subtracted from total measured monoterpenes. We limit our analysis to between 6:00 and 7:00 a.m. LT which reflects anticipated times of co-emission and minimal amounts of photochemical aging. Indeed, $[M_{anthro}/B]_{observed}$ is highest in our dataset during this time. The monthly average of $[M_{anthro}/B]_{observed}$ is 1.75 (July) and 1.95 (December). FIVE-VCP agrees better with our NNMF-apportioned monoterpenes measurements, with estimated $ER_{M/B\_FIVE\text{-}VCP}$ values at 1.02 in July and 2.02 in December, while NEI16 significantly underestimates $[M_{anthro}/B]$ during both seasons (July: 0.49, December: 0.78). The higher ratios for FIVE-VCP could reflect the higher estimate of VCP emission factor at ~42 kg per person per year, comparing to NEI's estimate of ~8 kg per person per year (Qin et al., 2020; McDonald et al., 2018). In addition, the diurnal emission profile of personal care products established in FIVE-VCP with a significant morning peak may better characterize the emission trends of monoterpenes (Coggon et al., 2021), which is demonstrated in our analysis. For the NNMF-apportioned PTR-ToF-MS ratios, we estimate a 10% uncertainty from the NNMF analysis (Sect. S2.4), with an additional overestimation in anthropogenic monoterpenes of up to 20% (Sect. 3.2). For FIVE-VCP, we estimate an uncertainty of 25% in anthropogenic monoterpenes and 30% in benzene, consistent with previously reported uncertainties of these species (Coggon et al., 2021; McDonald et al., 2018).

Our observed $[M_{anthro}/B]$ exceeds the emission inventory $ER_{M/B}$ estimates in all but one scenario (FIVE-VCP, December), but still within

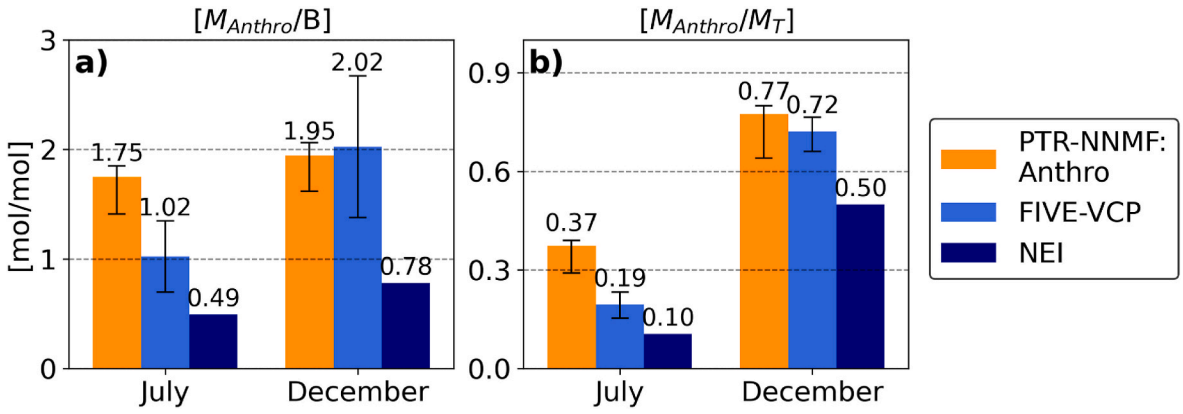

Fig. 8. Comparison of (a) anthropogenic monoterpenes-to-benzene ratio between NNMF speciated PTR measurements, FIVE-VCP, and NEI, and (b) anthropogenic-to-total monoterpenes ratio between NNMF sources, using MEGAN for biogenic emission estimates, during two different seasons between 6 and 7 a.m. NNMF error bar ranges reflect the 10% uncertainty in factorization and likely mis-apportionment of up to 20% of all monoterpenes to anthropogenic sources. FIVE-VCP has an estimated 25–30% uncertainty depending on the species.

the 10% uncertainty of our NNMF analysis that apportions anthropogenic monoterpenes. FIVE-VCP agrees well with NEI16 on benzene emissions, and previous studies using the NEI and various CTMs have found modeled benzene mixing ratios to be equal to or slightly less than field measurements (Scheffe et al., 2016; Hu et al., 2015). Thus, it is less likely that both models would overpredict benzene in this analysis. Monoterpenes are known to be underestimated in emission inventories. Sources of anthropogenic monoterpenes, especially products from urban consumer usage that are not well-represented in the NEI, would substantially impact the estimated $ER_{M/B}$ and is likely the most plausible source of discrepancies between observations and inventory estimates. Overall, the FIVE-VCP agrees better with NNMF anthropogenic monoterpenes-to-benzene ratio within 50% in the summer and within 10% in the winter. As suggested by Coggon et al. (2021), the larger difference between summer observations and FIVE-VCP estimates may be a result of VCP sources currently unaccounted for in the FIVE-VCP inventory, including emissions from constructions and building materials. The temperature dependence of such evaporative emissions would impact summertime estimates more significantly, thus creating the discrepancies between the seasons as presented here.

4.2. Anthropogenic-to-total monoterpenes using MEGAN

We also compare anthropogenic-to-total measured monoterpenes ratio, $[M_{anthro}/M_T]$, between observed NNMF results with the ratios using emission inventories. We consider factors 1 and 2 of our NNMF to be biogenic, and factors 3 through 6 to be from primary anthropogenic sources. Factors 7 and 8 are characterized as secondary based on speciation and seasonality patterns and are excluded from this comparison. MEGAN is used to estimate biogenic emission of monoterpenes, and total monoterpene emissions is equal to the sum of biogenic emissions using MEGAN and anthropogenic emissions of either NEI16 or FIVE-VCP. We compare monthly averages of July and December between 6 a.m. and 7 a.m. analogous to the method used in Sect. 4.1 (Fig. 8b). We expect anthropogenic monoterpene emissions to be higher and oxidation to be slower in the morning than during the day, allowing a better comparison between measurements and emission estimates. NNMF results show a slight decrease of anthropogenic monoterpenes in December at 0.26 ppb vs. 0.31 ppb in July. Biogenic factors decreased significantly from 0.76 ppb (July) to 0.09 ppb (December). $[M_{anthro}/M_T]_{observed}$ is 0.37 (July) and 0.77 (November). Biogenic emissions from MEGAN decreased by over 90% from 5.07×10^{-10} mol m^{-2} s^{-1} in July to 4.70×10^{-11} mol m^{-2} s^{-1} in December, while anthropogenic emissions remained relatively steady between seasons for both NEI16 and FIVE-VCP within 20%. As a result, $[M_{anthro}/M_T]$ of both inventories are higher in the winter. For FIVE-VCP with MEGAN, the ratio increased from 0.19 (July) to 0.72 (December), and for NEI with MEGAN from 0.10 (July) to 0.50 (December). NEI16 anthropogenic emissions from 6 a.m. to 7 a.m. in July (5.89×10^{-11} mol m^{-2} s^{-1}) is less than 50% of that of FIVE-VCP (1.22×10^{-10} mol m^{-2} s^{-1}).

The better agreement in the winter between measurements and anthropogenic inventory estimates in both $[M_{anthro}/B]$ and $[M_{anthro}/M_T]$ may partially be explained by the uncertainties associated with biogenic emissions, in the NNMF source apportionment and in the MEGAN emission estimates. For MEGAN, we selected a spatial resolution of 12 km for all three inventories for consistency, and while this resolution may account for transport effects, overestimation in biogenic monoterpenes is plausible as our measurement site is immediately surrounded by urban developments with the least amount of foliage coverage than the rest of the grid cell. Regarding the NNMF apportionment, the temporal correlation of monoterpenes to the traffic and cooking/biomass burning factors (factors 3–5) results in a total of 9% ± 3% of all monoterpenes being mis-apportioned to these factors. Neither of the sectors is a significant source of monoterpenes and part or all of the monoterpenes apportioned to these factors may be of biogenic origin, which may help explain the discrepancy between observed data and inventory estimates. Overall, FIVE-VCP again agrees better with NNMF-apportioned observations of anthropogenic-to-total monoterpenes within 50%, especially in the winter with <10% difference, while the NEI underestimates anthropogenic emissions of monoterpenes by as much as 70% in the summer.

5. Implications

Our analysis provides the first observational evidence that in the urban SE US, a biogenic-rich region, VCP emissions contribute to ambient monoterpene concentrations. Our data suggests that by summer 2020, anthropogenic emissions in Atlanta are comparable to non-pandemic levels. This suggests that VCPs contribute to summertime SOA formation in the region under previous and future "typical" emission scenarios unaffected by COVID-19. Zhang et al. (2018) have estimated that monoterpenes contribute to as much as 50% to total summertime SOA in the SE US, although assuming most monoterpenes are emitted from biogenic sources. If 35% of monoterpenes in the summer are anthropogenic as shown by our NNMF, and 26% out of which are from VCP-related sources, then ~17% of SOA could instead be traced back to local anthropogenic sources with at least 13% directly from VCP sources, excluding any potential influence from regional transport of biogenic SOA. While wintertime atmospheric chemistry differs from the warmer months with much less SOA formation,

observations in other regions of the world suggest wintertime SOAs may not be negligible and could still impact atmospheric chemistry and human health (Schroder et al., 2018). Our estimates of wintertime VCP monoterpene emissions by as much as 53% in the city would impact how the sources and fate of monoterpenes need to be evaluated especially in urban Atlanta during all seasons.

Most studies and models use α-pinene or β-pinene in evaluating the OH reactivity and SOA or O_3 formation of monoterpenes. While biogenic emissions of monoterpenes in the region is dominated by the pinenes (Geron et al., 2000), limonene is often found in VCP products (Steinemann, 2016) and has been shown as the dominant monoterpene species in an urban downtown core (Gkatzelis et al., 2021a). Chamber studies suggest that the SOA yield of limonene is over 6 times higher than that of α-pinene, at 16.9% for limonene and only 2.5% for α-pinene (Zhao et al., 2015). Therefore, anthropogenic monoterpenes would significantly impact the SOA formation process especially in densely populated areas in Atlanta. Additionally, for the 3 most-common monoterpenes species, limonene has the highest OH reaction rate constant almost 3 times as much as that of α-pinene or β-pinene (Atkinson, 1997). Limonene with the shortest lifetime and highest abundance in consumer products would significantly impact the atmospheric reactivity in urban Atlanta, and also affect SOA and O_3 formation that is likely underestimated than using the less reactive α-pinene or β-pinene.

The uncertainties in the PTR-ToF-MS measurements and NNMF analysis are influenced by instrumentation and calibration limitations (e.g., 10%–50% depending on species and sensitivity), uncertainties in factor selection and identification (e.g., NNMF uncertainty of 10%), and the likely mis-apportionment of factors due to temporal correlation (e.g., up to 20% of monoterpenes apportioned to biomass burning and secondary sources). The spatiotemporal variability in biogenic and anthropogenic monoterpenes adds additional uncertainties in inventories and models that can be on the order of a factor of two on a regional scale and even higher at a finer resolution needed to explore emissions and exposure on a city or sub-city level (Jiang et al., 2019; Carlton and Baker, 2011). A limited number of observations with species and temporal resolution suitable for comparison provides further challenge in the evaluation and verification of such emission data within the US over an extended period of time (Seltzer et al., 2021; McDonald et al., 2018). Future analysis on speciation of monoterpenes in the region and updated models with a more accurate speciation may provide quantifiable improvements of anthropogenic monoterpene emission estimates, with implications of VCP-related emissions on regional air quality.

6. Conclusions

Our observations indicate that anthropogenic monoterpene emissions, especially from VCP sources, have been underestimated in emissions inventories and models for Atlanta. NNMF source apportionment analysis of 7 months of PTR-ToF-MS data indicates that VCP emissions contribute to at least 26% of total monoterpene emissions in the summer, increasing to 53% in the winter. Evidence support our NNMF to be representative of the source analysis on VOCs in Atlanta, and the large contribution from anthropogenic sources especially in the winter is reflected in our factorization analysis that shows excellent agreement with the measurements. The temporal correlation between monoterpenes and other tracers such as D5-siloxane or ethanol further signifies the importance of VCP sources of monoterpenes in urban air, consistent with analyses on monoterpenes in other major cities within the US (Coggon et al., 2021; Gkatzelis et al., 2021b). Activity data and interannual comparison suggest minimal impact of the COVID-19 pandemic on our dataset, and the measurements and source apportionment analyses are reflective of a "typical" year in Atlanta.

Monoterpenes have been shown in this work as a VCP tracer in Atlanta with strong correlations to human activities, which are not accounted for in many traditional emission inventories, presenting a need to update such inventories especially in urban areas to better account for anthropogenic monoterpenes. Comparison of morning monoterpenes-to-benzene and anthropogenic-to-total-monoterpenes measurement ratios with the NEI16 and FIVE-VCP emission inventories show that FIVE-VCP has better agreements with measurement data in both July and December, while anthropogenic monoterpenes are likely still undercounted in the NEI16 platform in Atlanta by at least 50%. These findings imply that the FIVE-VCP may be more accurately assessing impact of anthropogenic activities and VCP emissions on atmospheric chemistry, especially in the winter, while summertime estimates can be affected by uncertainties in biogenic emissions and possible emissions from sectors still unaccounted for in both inventories.

Considering the significant potential contributions of monoterpenes to SOA formation in Atlanta, additional VOC flux measurements rather than concentrations, such as ones used in Karl et al. (2018), can address the impact of meteorology on observations and provide evaluations on an emission-constrained VOC profile. Additional background VOC measurements or speciated monoterpenes measurements are both valuable tools that can help quantitatively assess VCP contribution of monoterpenes, providing further insights on anthropogenic emissions of monoterpenes in Atlanta. Finally, additional analysis using high-resolution CTMs can help evaluate the accuracy of current emission inventories and their impact on SOA formation, and help quantifying impacts of VCPs on regional air quality.

CRediT authorship contribution statement

Yuyang Peng: Conceptualization, Methodology, Validation, Formal analysis, Investigation, Data curation, Writing – original draft, Writing – review & editing, Visualization. **Asher P. Mouat:** Investigation, Data curation. **Yongtao Hu:** Investigation, Data curation, Writing – review & editing. **Meng Li:** Investigation, Data curation, Writing – review & editing. **Brian C. McDonald:** Investigation, Data curation, Writing – review & editing. **Jennifer Kaiser:** Conceptualization, Methodology, Validation, Formal analysis, Supervision, Project administration, Funding acquisition, Visualization, Writing - review & editing.

Declaration of competing interest

The authors declare that they have no known competing financial interests or personal relationships that could have appeared to influence the work reported in this paper.

Data availability

Data will be made available on request.

Acknowledgements

This study was supported by the NOAA Climate Program Office's Atmospheric Chemistry, Carbon Cycle, and Climate program (grant NA21OAR4310221), NASA (grant 80NSSC21K0506), and the US EPA (grant 84024601). The contents of this study are solely the responsibility of the grantee, and do not necessarily represent the official views of the supporting agencies.

Appendix A. Supplementary data

Supplementary data to this article can be found online at https://doi.org/10.1016/j.atmosenv.2022.119324.

References

Abdullahi, K.L., Delgado-Saborit, J.M., Harrison, R.M., 2013. Emissions and indoor concentrations of particulate matter and its specific chemical components from cooking: a review. Atmos. Environ. 71, 260–294. https://doi.org/10.1016/j.atmosenv.2013.01.061.

Atkinson, R., 1997. Gas-Phase tropospheric chemistry of volatile organic compounds: 1. Alkanes and alkenes. J. Phys. Chem. Ref. Data 26, 215–290. https://doi.org/10.1063/1.556012.

Atkinson, R., Baulch, D.L., Cox, R.A., Crowley, J.N., Hampson, R.F., Hynes, R.G., Jenkin, M.E., Rossi, M.J., Troe, J., Subcommittee, I., 2006. Evaluated kinetic and photochemical data for atmospheric chemistry: volume II – gas phase reactions of organic species. Atmos. Chem. Phys. 6, 3625–4055. https://doi.org/10.5194/acp-6-3625-2006.

Biesenthal, T.A., Shepson, P.B., 1997. Observations of anthropogenic inputs of the isoprene oxidation products methyl vinyl ketone and methacrolein to the atmosphere. Geophys. Res. Lett. 24, 1375–1378. https://doi.org/10.1029/97GL01337.

Borbon, A., Gilman, J.B., Kuster, W.C., Grand, N., Chevaillier, S., Colomb, A., Dolgorouky, C., Gros, V., Lopez, M., Sarda-Esteve, R., Holloway, J., Stutz, J., Petetin, H., McKeen, S., Beekmann, M., Warneke, C., Parrish, D.D., de Gouw, J.A., 2013. Emission ratios of anthropogenic volatile organic compounds in northern mid-latitude megacities: observations versus emission inventories in Los Angeles and Paris. J. Geophys. Res. Atmos. 118, 2041–2057. https://doi.org/10.1002/jgrd.50059.

Borduas, N., da Silva, G., Murphy, J.G., Abbatt, J.P.D., 2015. Experimental and theoretical understanding of the gas phase oxidation of atmospheric amides with OH radicals: kinetics, products, and mechanisms. J. Phys. Chem. 119, 4298–4308. https://doi.org/10.1021/jp503759f.

Brewer, J.F., Bishop, M., Kelp, M., Keller, C.A., Ravishankara, A.R., Fischer, E.V., 2017. A sensitivity analysis of key natural factors in the modeled global acetone budget. J. Geophys. Res. Atmos. 122, 2043–2058. https://doi.org/10.1002/2016jd025935.

Butler, T.M., Lawrence, M.G., Taraborrelli, D., Lelieveld, J., 2011. Multi-day ozone production potential of volatile organic compounds calculated with a tagging approach. Atmos. Environ. 45, 4082–4090. https://doi.org/10.1016/j.atmosenv.2011.03.040.

Carlton, A.G., Baker, K.R., 2011. Photochemical modeling of the Ozark isoprene volcano: MEGAN, BEIS, and their impacts on air quality predictions. Environ. Sci. Technol. 45, 4438–4445. https://doi.org/10.1021/es200050x.

Coggon, M.M., McDonald, B.C., Vlasenko, A., Veres, P.R., Bernard, F., Koss, A.R., Yuan, B., Gilman, J.B., Peischl, J., Aikin, K.C., DuRant, J., Warneke, C., Li, S.M., de Gouw, J.A., 2018. Diurnal variability and emission pattern of decamethylcyclopentasiloxane (D5) from the application of personal care products in two north American cities. Environ. Sci. Technol. 52, 5610–5618. https://doi.org/10.1021/acs.est.8b00506.

Coggon, M.M., Gkatzelis, G.I., McDonald, B.C., Gilman, J.B., Schwantes, R.H., Abuhassan, N., Aikin, K.C., Arend, M.F., Berkoff, T.A., Brown, S.S., Campos, T.L., Dickerson, R.R., Gronoff, G., Hurley, J.F., Isaacman-VanWertz, G., Koss, A.R., Li, M., McKeen, S.A., Moshary, F., Peischl, J., Pospisilova, V., Ren, X., Wilson, A., Wu, Y., Trainer, M., Warneke, C., 2021. Volatile chemical product emissions enhance ozone and modulate urban chemistry. Proc. Natl. Acad. Sci. U. S. A. 118 https://doi.org/10.1073/pnas.2026653118.

de Gouw, J.A., Gilman, J.B., Borbon, A., Warneke, C., Kuster, W.C., Goldan, P.D., Holloway, J.S., Peischl, J., Ryerson, T.B., Parrish, D.D., Gentner, D.R., Goldstein, A. H., Harley, R.A., 2012. Increasing atmospheric burden of ethanol in the United States. Geophys. Res. Lett. 39 https://doi.org/10.1029/2012gl052109.

de Gouw, J.A., Gilman, J.B., Kim, S.W., Alvarez, S.L., Dusanter, S., Graus, M., Griffith, S. M., Isaacman-VanWertz, G., Kuster, W.C., Lefer, B.L., Lerner, B.M., McDonald, B.C., Rappenglück, B., Roberts, J.M., Stevens, P.S., Stutz, J., Thalman, R., Veres, P.R., Volkamer, R., Warneke, C., Washenfelder, R.A., Young, C.J., 2018. Chemistry of volatile organic compounds in the Los Angeles Basin: formation of oxygenated compounds and determination of emission ratios. J. Geophys. Res. Atmos. 123, 2298–2319. https://doi.org/10.1002/2017jd027976.

Fisher, J.A., Jacob, D.J., Travis, K.R., Kim, P.S., Marais, E.A., Miller, C.C., Yu, K., Zhu, L., Yantosca, R.M., Sulprizio, M.P., Mao, J., Wennberg, P.O., Crounse, J.D., Teng, A.P., Nguyen, T.B., St Clair, J.M., Cohen, R.C., Romer, P., Nault, B.A., Wooldridge, P.J., Jimenez, J.L., Campuzano-Jost, P., Day, D.A., Hu, W., Shepson, P.B., Xiong, F., Blake, D.R., Goldstein, A.H., Misztal, P.K., Hanisco, T.F., Wolfe, G.M., Ryerson, T.B., Wisthaler, A., Mikoviny, T., 2016. Organic nitrate chemistry and its implications for nitrogen budgets in an isoprene- and monoterpene-rich atmosphere: constraints from aircraft (SEAC(4)RS) and ground-based (SOAS) observations in the Southeast US. Atmos. Chem. Phys. 16, 5969–5991. https://doi.org/10.5194/acp-16-5969-2016.

Fu, T.-M., Jacob, D.J., Wittrock, F., Burrows, J.P., Vrekoussis, M., Henze, D.K., 2008. Global budgets of atmospheric glyoxal and methylglyoxal, and implications for formation of secondary organic aerosols. J. Geophys. Res. Atmos. 113 https://doi.org/10.1029/2007JD009505.

Geron, C., Rasmussen, R., Arnts, R.R., Guenther, A., 2000. A review and synthesis of monoterpene speciation from forests in the United States. Atmos. Environ. 34, 1761–1781. https://doi.org/10.1016/S1352-2310(99)00364-7.

Gkatzelis, G.I., Coggon, M.M., McDonald, B.C., Peischl, J., Aikin, K.C., Gilman, J.B., Trainer, M., Warneke, C., 2021a. Identifying volatile chemical product tracer compounds in U.S. Cities. Environ. Sci. Technol. 55, 188–199. https://doi.org/10.1021/acs.est.0c05467.

Gkatzelis, G.I., Coggon, M.M., McDonald, B.C., Peischl, J., Gilman, J.B., Aikin, K.C., Robinson, M.A., Canonaco, F., Prevot, A.S.H., Trainer, M., Warneke, C., 2021b. Observations confirm that volatile chemical products are a major source of petrochemical emissions in U.S. Cities. Environ. Sci. Technol. 55, 4332–4343. https://doi.org/10.1021/acs.est.0c05471.

Goldan, P.D., Kuster, W.C., Fehsenfeld, F.C., Montzka, S.A., 1995. Hydrocarbon measurements in the southeastern United States: the rural oxidants in the southern environment (ROSE) program 1990. J. Geophys. Res. Atmos. 100, 25945–25963. https://doi.org/10.1029/95JD02607.

Guenther, A., Karl, T., Harley, P., Wiedinmyer, C., Palmer, P.I., Geron, C., 2006. Estimates of global terrestrial isoprene emissions using MEGAN (model of emissions of gases and aerosols from nature). Atmos. Chem. Phys. 6, 3181–3210. https://doi.org/10.5194/acp-6-3181-2006.

Guenther, A.B., Jiang, X., Heald, C.L., Sakulyanontvittaya, T., Duhl, T., Emmons, L.K., Wang, X., 2012. The Model of Emissions of Gases and Aerosols from Nature version 2.1 (MEGAN2.1): an extended and updated framework for modeling biogenic emissions. Geosci. Model Dev. (GMD) 5, 1471–1492. https://doi.org/10.5194/gmd-5-1471-2012.

Hantson, S., Knorr, W., Schurgers, G., Pugh, T.A.M., Arneth, A., 2017. Global isoprene and monoterpene emissions under changing climate, vegetation, CO 2 and land use. Atmos. Environ. 155, 35–45. https://doi.org/10.1016/j.atmosenv.2017.02.010.

Harkins, C., McDonald, B.C., Henze, D.K., Wiedinmyer, C., 2021. A fuel-based method for updating mobile source emissions during the COVID-19 pandemic. Environ. Res. Lett. 16, 065018 https://doi.org/10.1088/1748-9326/ac0660.

Harrison, S.P., Morfopoulos, C., Dani, K.G., Prentice, I.C., Arneth, A., Atwell, B.J., Barkley, M.P., Leishman, M.R., Loreto, F., Medlyn, B.E., Niinemets, U., Possell, M., Penuelas, J., Wright, I.J., 2013. Volatile isoprenoid emissions from plastid to planet. New Phytol. 197, 49–57. https://doi.org/10.1111/nph.12021.

Hoyle, C.R., Boy, M., Donahue, N.M., Fry, J.L., Glasius, M., Guenther, A., Hallar, A.G., Huff Hartz, K., Petters, M.D., Petäjä, T., Rosenoern, T., Sullivan, A.P., 2011. A review of the anthropogenic influence on biogenic secondary organic aerosol. Atmos. Chem. Phys. 11, 321–343. https://doi.org/10.5194/acp-11-321-2011.

Hu, L., Millet, D.B., Baasandorj, M., Griffis, T.J., Travis, K.R., Tessum, C.W., Marshall, J. D., Reinhart, W.F., Mikoviny, T., Müller, M., Wisthaler, A., Graus, M., Warneke, C., de Gouw, J., 2015. Emissions of C6–C8 aromatic compounds in the United States: constraints from tall tower and aircraft measurements. J. Geophys. Res. Atmos. 120, 826–842. https://doi.org/10.1002/2014JD022627.

Hu, Y., Ai, H.H., Odman, M.T., Vaidyanathan, A., Russell, A.G., 2019. Development of a WebGIS-based analysis tool for human health protection from the impacts of prescribed fire smoke in southeastern USA. Int. J. Environ. Res. Publ. Health 16. https://doi.org/10.3390/ijerph16111981.

Huang, G., Ponder, R., Bond, A., Brim, H., Temeng, A., Naeger, A.R., Zhu, L., 2021. Unexpected impact of COVID-19 lockdown on the air quality in the metro Atlanta, USA using ground-based and satellite observations. Aerosol Air Qual. Res. 21, 210153 https://doi.org/10.4209/aaqr.210153.

Huangfu, Y., Yuan, B., Wang, S., Wu, C., He, X., Qi, J., de Gouw, J., Warneke, C., Gilman, J.B., Wisthaler, A., Karl, T., Graus, M., Jobson, B.T., Shao, M., 2021. Revisiting acetonitrile as tracer of biomass burning in anthropogenic-influenced environments. Geophys. Res. Lett. 48, e2020GL092322 https://doi.org/10.1029/2020GL092322.

Jacob, D.J., Field, B.D., Jin, E.M., Bey, I., Li, Q., Logan, J.A., Yantosca, R.M., Singh, H.B., 2002. Atmospheric budget of acetone. J. Geophys. Res. Atmos. 107 https://doi.org/10.1029/2001jd000694. ACH 5-1-ACH 5-17.

Jiang, J., Aksoyoglu, S., Ciarelli, G., Oikonomakis, E., El-Haddad, I., Canonaco, F., O'Dowd, C., Ovadnevaite, J., Minguillón, M.C., Baltensperger, U., Prévôt, A.S.H., 2019. Effects of two different biogenic emission models on modelled ozone and aerosol concentrations in Europe. Atmos. Chem. Phys. 19, 3747–3768. https://doi.org/10.5194/acp-19-3747-2019.

Jiang, Z., McDonald Brian, C., Worden, H., Worden John, R., Miyazaki, K., Qu, Z., Henze Daven, K., Jones Dylan, B.A., Arellano Avelino, F., Fischer Emily, V., Zhu, L., Boersma, K.F., 2018. Unexpected slowdown of US pollutant emission reduction in the past decade. Proc. Natl. Acad. Sci. USA 115, 5099–5104. https://doi.org/10.1073/pnas.1801191115.

Jordan, A., Haidacher, S., Hanel, G., Hartungen, E., Märk, L., Seehauser, H., Schottkowsky, R., Sulzer, P., Märk, T.D., 2009. A high resolution and high sensitivity proton-transfer-reaction time-of-flight mass spectrometer (PTR-TOF-MS). Int. J. Mass Spectrom. 286, 122–128. https://doi.org/10.1016/j.ijms.2009.07.005.

Karl, T., Striednig, M., Graus, M., Hammerle, A., Wohlfahrt, G., 2018. Urban flux measurements reveal a large pool of oxygenated volatile organic compound emissions. Proc. Natl. Acad. Sci. U. S. A. 115, 1186–1191. https://doi.org/10.1073/pnas.1714715115.

Karl, T.G., Christian, T.J., Yokelson, R.J., Artaxo, P., Hao, W.M., Guenther, A., 2007. The Tropical Forest and Fire Emissions Experiment: method evaluation of volatile organic compound emissions measured by PTR-MS, FTIR, and GC from tropical biomass burning. Atmos. Chem. Phys. 7, 5883–5897. https://doi.org/10.5194/acp-7-5883-2007.

Kaser, L., Peron, A., Graus, M., Striednig, M., Wohlfahrt, G., Juráň, S., Karl, T., 2022. Interannual variability of terpenoid emissions in an alpine city. Atmos. Chem. Phys. 22, 5603–5618. https://doi.org/10.5194/acp-22-5603-2022.

Kim, P.S., Jacob, D.J., Fisher, J.A., Travis, K., Yu, K., Zhu, L., Yantosca, R.M., Sulprizio, M.P., Jimenez, J.L., Campuzano-Jost, P., Froyd, K.D., Liao, J., Hair, J.W., Fenn, M.A., Butler, C.F., Wagner, N.L., Gordon, T.D., Welti, A., Wennberg, P.O., Crounse, J.D., St, Clair, J.M., Teng, A.P., Millet, D.B., Schwarz, J.P., Markovic, M.Z., Perring, A.E., 2015. Sources, seasonality, and trends of southeast US aerosol: an integrated analysis of surface, aircraft, and satellite observations with the GEOS-Chem chemical transport model. Atmos. Chem. Phys. 15, 10411–10433. https://doi.org/10.5194/acp-15-10411-2015.

Klein, F., Platt, S.M., Farren, N.J., Detournay, A., Bruns, E.A., Bozzetti, C., Daellenbach, K.R., Kilic, D., Kumar, N.K., Pieber, S.M., Slowik, J.G., Temime-Roussel, B., Marchand, N., Hamilton, J.F., Baltensperger, U., Prevot, A.S., El Haddad, I., 2016. Characterization of gas-phase organics using proton transfer reaction time-of-flight mass spectrometry: cooking emissions. Environ. Sci. Technol. 50, 1243–1250. https://doi.org/10.1021/acs.est.5b04618.

Kondragunta, S., Wei, Z., McDonald, B.C., Goldberg, D.L., Tong, D.Q., 2021. COVID-19 induced fingerprints of a new normal urban air quality in the United States.

J. Geophys. Res. Atmos. 126, e2021JD034797 https://doi.org/10.1029/2021JD034797.
Link, M.F., Brophy, P., Fulgham, S.R., Murschell, T., Farmer, D.K., 2021. Isoprene versus monoterpenes as gas-phase organic acid precursors in the atmosphere. ACS Earth and Space Chemistry 5, 1600–1612. https://doi.org/10.1021/acsearthspacechem.1c00093.
McDonald, B.C., de Gouw, J.A., Gilman, J.B., Jathar, S.H., Akherati, A., Cappa, C.D., Jimenez, J.L., Lee-Taylor, J., Hayes, P.L., McKeen, S.A., Cui, Y.Y., Kim, S.W., Gentner, D.R., Isaacman-VanWertz, G., Goldstein, A.H., Harley, R.A., Frost, G.J., Roberts, J.M., Ryerson, T.B., Trainer, M., 2018. Volatile chemical products emerging as largest petrochemical source of urban organic emissions. Science 359, 760–764. https://doi.org/10.1126/science.aaq0524.
McGlynn, D.F., Barry, L.E.R., Lerdau, M.T., Pusede, S.E., Isaacman-VanWertz, G., 2021. Measurement report: variability in the composition of biogenic volatile organic compounds in a Southeastern US forest and their role in atmospheric reactivity. Atmos. Chem. Phys. 21, 15755–15770. https://doi.org/10.5194/acp-21-15755-2021.
Merry, K., Siry, J., Bettinger, P., Bowker, J.M., 2014. Urban tree cover change in Detroit and Atlanta, USA, 1951-2010. Cities 41, 123–131. https://doi.org/10.1016/j.cities.2014.06.012.
Monks, P.S., Archibald, A.T., Colette, A., Cooper, O., Coyle, M., Derwent, R., Fowler, D., Granier, C., Law, K.S., Mills, G.E., Stevenson, D.S., Tarasova, O., Thouret, V., von Schneidemesser, E., Sommariva, R., Wild, O., Williams, M.L., 2015. Tropospheric ozone and its precursors from the urban to the global scale from air quality to short-lived climate forcer. Atmos. Chem. Phys. 15, 8889–8973. https://doi.org/10.5194/acp-15-8889-2015.
Müller, M., Anderson, B.E., Beyersdorf, A.J., Crawford, J.H., Diskin, G.S., Eichler, P., Fried, A., Keutsch, F.N., Mikoviny, T., Thornhill, K.L., Walega, J.G., Weinheimer, A. J., Yang, M., Yokelson, R.J., Wisthaler, A., 2016. In situ measurements and modeling of reactive trace gases in a small biomass burning plume. Atmos. Chem. Phys. 16, 3813–3824. https://doi.org/10.5194/acp-16-3813-2016.
Paulot, F., Wunch, D., Crounse, J.D., Toon, G.C., Millet, D.B., DeCarlo, P.F., Vigouroux, C., Deutscher, N.M., Gonzalez Abad, G., Notholt, J., Warneke, T., Hannigan, J.W., Warneke, C., de Gouw, J.A., Dunlea, E.J., De Maziere, M., Griffith, D.W.T., Bernath, P., Jimenez, J.L., Wennberg, P.O., 2011. Importance of secondary sources in the atmospheric budgets of formic and acetic acids. Atmos. Chem. Phys. 11, 1989–2013. https://doi.org/10.5194/acp-11-1989-2011.
Porter, W.C., Safieddine, S.A., Heald, C.L., 2017. Impact of aromatics and monoterpenes on simulated tropospheric ozone and total OH reactivity. Atmos. Environ. 169, 250–257. https://doi.org/10.1016/j.atmosenv.2017.08.048.
Pye, H.O.T., Luecken, D.J., Xu, L., Boyd, C.M., Ng, N.L., Baker, K.R., Ayres, B.R., Bash, J. O., Baumann, K., Carter, W.P.L., Edgerton, E., Fry, J.L., Hutzell, W.T., Schwede, D.B., Shepson, P.B., 2015. Modeling the current and future roles of particulate organic nitrates in the southeastern United States. Environ. Sci. Technol. 49, 14195–14203. https://doi.org/10.1021/acs.est.5b03738.
Qin, M., Hu, Y., Wang, X., Vasilakos, P., Boyd, C.M., Xu, L., Song, Y., Ng, N.L., Nenes, A., Russell, A.G., 2018. Modeling biogenic secondary organic aerosol (BSOA) formation from monoterpene reactions with NO3: a case study of the SOAS campaign using CMAQ. Atmos. Environ. 184, 146–155. https://doi.org/10.1016/j.atmosenv.2018.03.042.
Qin, M., Murphy, B.N., Isaacs, K.K., McDonald, B.C., Lu, Q., McKeen, S.A., Koval, L., Robinson, A.L., Efstathiou, C., Allen, C., Pye, H.O.T., 2020. Criteria pollutant impacts of volatile chemical products informed by near-field modeling. Nat Sustain, N/A 1–57. https://doi.org/10.1038/s41893-020-00614-1.
Sakulyanontvittaya, T., Duhl, T., Wiedinmyer, C., Helmig, D., Matsunaga, S., Potosnak, M., Milford, J., Guenther, A., 2008. Monoterpene and sesquiterpene emission estimates for the United States. Environ. Sci. Technol. 42, 1623–1629. https://doi.org/10.1021/es702274e.
Scheffe, R.D., Strum, M., Phillips, S.B., Thurman, J., Eyth, A., Fudge, S., Morris, M., Palma, T., Cook, R., 2016. Hybrid modeling approach to estimate exposures of hazardous air pollutants (HAPs) for the national air toxics assessment (NATA). Environ. Sci. Technol. 50, 12356–12364. https://doi.org/10.1021/acs.est.6b04752.
Schieweck, A., Uhde, E., Salthammer, T., 2021. Determination of acrolein in ambient air and in the atmosphere of environmental test chambers. Environ. Sci. J. Integr. Environ. Res.: Process. Impacts 23, 1729–1746. https://doi.org/10.1039/D1EM00221J.
Schroder, J.C., Campuzano-Jost, P., Day, D.A., Shah, V., Larson, K., Sommers, J.M., Sullivan, A.P., Campos, T., Reeves, J.M., Hills, A., Hornbrook, R.S., Blake, N.J., Scheuer, E., Guo, H., Fibiger, D.L., McDuffie, E.E., Hayes, P.L., Weber, R.J., Dibb, J. E., Apel, E.C., Jaeglé, L., Brown, S.S., Thornton, J.A., Jimenez, J.L., 2018. Sources and secondary production of organic aerosols in the northeastern United States during WINTER. J. Geophys. Res. Atmos. 123, 7771–7796. https://doi.org/10.1029/2018JD028475.
Sekimoto, K., Li, S.-M., Yuan, B., Koss, A., Coggon, M., Warneke, C., de Gouw, J., 2017. Calculation of the sensitivity of proton-transfer-reaction mass spectrometry (PTR-MS) for organic trace gases using molecular properties. Int. J. Mass Spectrom. 421, 71–94. https://doi.org/10.1016/j.ijms.2017.04.006.
Seltzer, K.M., Pennington, E., Rao, V., Murphy, B.N., Strum, M., Isaacs, K.K., Pye, H.O.T., 2021. Reactive organic carbon emissions from volatile chemical products. Atmos. Chem. Phys. 21, 5079–5100. https://doi.org/10.5194/acp-21-5079-2021.
Shilling, J.E., Zaveri, R.A., Fast, J.D., Kleinman, L., Alexander, M.L., Canagaratna, M.R., Fortner, E., Hubbe, J.M., Jayne, J.T., Sedlacek, A., Setyan, A., Springston, S., Worsnop, D.R., Zhang, Q., 2013. Enhanced SOA formation from mixed anthropogenic and biogenic emissions during the CARES campaign. Atmos. Chem. Phys. 13, 2091–2113. https://doi.org/10.5194/acp-13-2091-2013.
Shrivastava, M., Andreae, M.O., Artaxo, P., Barbosa, H.M.J., Berg, L.K., Brito, J., Ching, J., Easter, R.C., Fan, J., Fast, J.D., Feng, Z., Fuentes, J.D., Glasius, M., Goldstein, A.H., Alves, E.G., Gomes, H., Gu, D., Guenther, A., Jathar, S.H., Kim, S., Liu, Y., Lou, S., Martin, S.T., McNeill, V.F., Medeiros, A., de Sa, S.S., Shilling, J.E., Springston, S.R., Souza, R.A.F., Thornton, J.A., Isaacman-VanWertz, G., Yee, L.D., Ynoue, R., Zaveri, R.A., Zelenyuk, A., Zhao, C., 2019. Urban pollution greatly enhances formation of natural aerosols over the Amazon rainforest. Nat. Commun. 10, 1046. https://doi.org/10.1038/s41467-019-08909-4.
Simoneit, B.R.T., 2002. Biomass burning — a review of organic tracers for smoke from incomplete combustion. Appl. Geochem. 17, 129–162. https://doi.org/10.1016/S0883-2927(01)00061-0.
Steinemann, A., 2016. Fragranced consumer products: exposures and effects from emissions. Air Qual Atmos Health 9, 861–866. https://doi.org/10.1007/s11869-016-0442-z.
Steiner, A.L., Tonse, S., Cohen, R.C., Goldstein, A.H., Harley, R.A., 2007. Biogenic 2-methyl-3-buten-2-ol increases regional ozone and HOx sources. Geophys. Res. Lett. 34 https://doi.org/10.1029/2007GL030802.
Stoica, P., Selen, Y., 2004. Model-order selection: a review of information criterion rules. IEEE Signal Process. Mag. 21, 36–47. https://doi.org/10.1109/MSP.2004.1311138.
USEPA, 2021. Technical Support Document (TSD) Preparation of Emissions Inventories for the 2016v1. North American Emissions Modeling Platform.
Van Rooy, P., Tasnia, A., Barletta, B., Buenconsejo, R., Crounse, J.D., Kenseth, C.M., Meinardi, S., Murphy, S., Parker, H., Schulze, B., Seinfeld, J.H., Wennberg, P.O., Blake, D.R., Barsanti, K.C., 2021. Observations of volatile organic compounds in the Los Angeles Basin during COVID-19. ACS Earth and Space Chemistry 5, 3045–3055. https://doi.org/10.1021/acsearthspacechem.1c00248.
Warneke, C., McKeen, S.A., de Gouw, J.A., Goldan, P.D., Kuster, W.C., Holloway, J.S., Williams, E.J., Lerner, B.M., Parrish, D.D., Trainer, M., Fehsenfeld, F.C., Kato, S., Atlas, E.L., Baker, A., Blake, D.R., 2007. Determination of urban volatile organic compound emission ratios and comparison with an emissions database. J. Geophys. Res. Atmos. 112 https://doi.org/10.1029/2006jd007930.
Weber, R.J., Sullivan, A.P., Peltier, R.E., Russell, A., Yan, B., Zheng, M., de Gouw, J., Warneke, C., Brock, C., Holloway, J.S., Atlas, E.L., Edgerton, E., 2007. A study of secondary organic aerosol formation in the anthropogenic-influenced southeastern United States. J. Geophys. Res. Atmos. 112 https://doi.org/10.1029/2007JD008408.
Xu, L., Pye, H.O.T., He, J., Chen, Y., Murphy, B.N., Ng, L.N., 2018. Experimental and model estimates of the contributions from biogenic monoterpenes and sesquiterpenes to secondary organic aerosol in the southeastern United States. Atmos. Chem. Phys. 18, 12613–12637. https://doi.org/10.5194/acp-18-12613-2018.
Xu, L., Guo, H., Boyd, C.M., Klein, M., Bougiatioti, A., Cerully, K.M., Hite, J.R., Isaacman-VanWertz, G., Kreisberg, N.M., Knote, C., Olson, K., Koss, A., Goldstein, A.H., Hering, S.V., de Gouw, J., Baumann, K., Lee, S.-H., Nenes, A., Weber, R.J., Ng, N.L., 2015. Effects of anthropogenic emissions on aerosol formation from isoprene and monoterpenes in the southeastern United States. Proc. Natl. Acad. Sci. USA 112, 37–42.
Yeoman, A.M., Shaw, M., Carslaw, N., Murrells, T., Passant, N., Lewis, A.C., 2020. Simplified speciation and atmospheric volatile organic compound emission rates from non-aerosol personal care products. Indoor Air 30, 459–472. https://doi.org/10.1111/ina.12652.
Yuan, B., Shao, M., Lu, S., Wang, B., 2010. Source profiles of volatile organic compounds associated with solvent use in Beijing, China. Atmos. Environ. 44, 1919–1926. https://doi.org/10.1016/j.atmosenv.2010.02.014.
Yuan, B., Koss, A.R., Warneke, C., Coggon, M., Sekimoto, K., de Gouw, J.A., 2017. Proton-transfer-reaction mass spectrometry: applications in atmospheric sciences. Chem. Rev. 117, 13187–13229. https://doi.org/10.1021/acs.chemrev.7b00325.
Yuan, B., Shao, M., de Gouw, J., Parrish, D.D., Lu, S., Wang, M., Zeng, L., Zhang, Q., Song, Y., Zhang, J., Hu, M., 2012. Volatile organic compounds (VOCs) in urban air: how chemistry affects the interpretation of positive matrix factorization (PMF) analysis. J. Geophys. Res. Atmos. 117 https://doi.org/10.1029/2012JD018236.
Yuan, H., Dai, Y., Xiao, Z., Ji, D., Shangguan, W., 2011. Reprocessing the MODIS Leaf Area Index products for land surface and climate modelling. Remote Sensing of Environment - REM. SENS. ENVIRON. 115, 1171–1187. https://doi.org/10.1016/j.rse.2011.01.001.
Zhang, H., Yee, L.D., Lee, B.H., Curtis, M.P., Worton, D.R., Isaacman-VanWertz, G., Offenberg, J.H., Lewandowski, M., Kleindienst, T.E., Beaver, M.R., Holder, A.L., Lonneman, W.A., Docherty, K.S., Jaoui, M., Pye, H.O.T., Hu, W., Day, D.A., Campuzano-Jost, P., Jimenez, J.L., Guo, H., Weber, R.J., de Gouw, J., Koss, A.R., Edgerton, E.S., Brune, W., Mohr, C., Lopez-Hilfiker, F.D., Lutz, A., Kreisberg, N.M., Spielman, S.R., Hering, S.V., Wilson, K.R., Thornton, J.A., Goldstein, A.H., 2018. Monoterpenes are the largest source of summertime organic aerosol in the southeastern United States. Proc. Natl. Acad. Sci. U. S. A. 115, 2038–2043. https://doi.org/10.1073/pnas.1717513115.
Zhao, D.F., Kaminski, M., Schlag, P., Fuchs, H., Acir, I.H., Bohn, B., Häseler, R., Kiendler-Scharr, A., Rohrer, F., Tillmann, R., Wang, M.J., Wegener, R., Wildt, J., Wahner, A., Mentel, T.F., 2015. Secondary organic aerosol formation from hydroxyl radical oxidation and ozonolysis of monoterpenes. Atmos. Chem. Phys. 15, 991–1012. https://doi.org/10.5194/acp-15-991-2015.